

---

# NAVIGATION SERVICES AMPLIFY CONCENTRATION OF TRAFFIC AND EMISSIONS IN OUR CITIES

---

**Giuliano Cornacchia**

ISTI-CNR, Pisa, Italy

Department of Computer Science, Pisa, Italy

giuliano.cornacchia@isti.cnr.it

**Mirco Nanni**

ISTI-CNR, Pisa, Italy

mirco.nanni@isti.cnr.it

**Dino Pedreschi**

Department of Computer Science, Pisa, Italy

dino.pedreschi@unipi.it

**Luca Pappalardo**

ISTI-CNR, Pisa, Italy

Scuola Normale Superiore, Pisa, Italy

luca.pappalardo@isti.cnr.it

## ABSTRACT

The proliferation of human-AI ecosystems involving human interaction with algorithms, such as assistants and recommenders, raises concerns about large-scale social behaviour. Despite evidence of such phenomena across several contexts, the collective impact of GPS navigation services remains unclear: while beneficial to the user, they can also cause chaos if too many vehicles are driven through the same few roads. Our study employs a simulation framework to assess navigation services' influence on road network usage and CO<sub>2</sub> emissions. The results demonstrate a universal pattern of amplified conformity: increasing adoption rates of navigation services cause a reduction of route diversity of mobile travellers and increased concentration of traffic and emissions on fewer roads, thus exacerbating an unequal distribution of negative externalities on selected neighbourhoods. Although navigation services recommendations can help reduce CO<sub>2</sub> emissions when their adoption rate is low, these benefits diminish or even disappear when the adoption rate is high and exceeds a certain city- and service-dependent threshold. We summarize these discoveries in a non-linear function that connects the marginal increase of conformity with the marginal reduction in CO<sub>2</sub> emissions. Our simulation approach addresses the challenges posed by the complexity of transportation systems and the lack of data and algorithmic transparency.

## Introduction

The ascent of human-AI ecosystems in which humans interact with various forms of algorithms, including AI assistants and recommender systems (in short, recommenders), multiplies the possibility for the emergence of large-scale social behaviour, possibly with unintended consequences [38, 35, 46, 34]. The aggregation of many individually “good” recommendations may have unintended outcomes because human choices, influenced by these recommendations, interfere with each other on top of shared resources.

We have evidence of this phenomenon in various contexts [38, 34]. Personalised recommendations on social media help users deal with information overload, but may artificially amplify echo chambers, filter bubbles, and processes of radicalisation [42, 23, 40, 5, 47, 15, 13]. Profiling and targeted advertising may further increase inequality and monopolies, with the harms of perpetuating and amplifying biases, discriminations, and the “tragedy of the commons” [26, 32, 28]. Mobile applications providing pedestrians directions to avoid high-crime areas make users feel safer, but may make dangerous areas more isolated, thus favouring a further increase in crime [48, 11, 22].

Notwithstanding, the collective impact of other pervasive recommenders is still little understood. A notable example is commercial navigation services (e.g., TomTom, Google Maps). These services recommend routes to a destination, considering historical and dynamically changing traffic conditions. Despite their indubitable usefulness, especially when exploring an unfamiliar city, navigation services may also create chaos if too many drivers are directed on a few roads [30, 43, 19]. This was the case of Leonia, a small town in New Jersey, USA. In 2017, GPS navigation apps repeatedly rerouted drivers on congested highways through Leonia’s narrow streets, creating such congestion that people could not get out of their driveways [19, 43]. Leonia’s community is not alone: increasingly, many towns globally have been grappling with the local gridlock caused by well-intentioned navigation apps [21, 31].

Beyond the anecdote, existing research in this area yields findings that are often sparse and contradictory, and predominantly focused on specific navigation services and individual cities [38, 35, 34, 16, 4]. Navigation services demonstrate potential in mitigating CO<sub>2</sub> and NO<sub>x</sub> emissions [7, 1, 4, 45, 39], reducing travel times [4], energy consumption [7], fuel usage [1], vehicle miles travelled [44], and accident risk [25]. However, they may also increase travel time, population exposure to NO<sub>x</sub> and traffic volume in some areas [45, 39], as well as redirect highway traffic onto city streets, parks, tourist destinations, and slower roads, thereby exacerbating local congestion [44, 25]. Overall, we lack robust studies to fully understand the multifaceted impact of navigation services on some externalities, such as road network usage and urban emissions. For example, what would the urban impacts of various navigation services be under different traffic conditions and adoption rates?

In this article, we provide two contributions to this intriguing debate. First, we design a simulation framework to evaluate the influence of navigation services on the urban environment regarding road network usage and CO<sub>2</sub> emissions. Our open-source framework is a realistic digital twin of urban traffic that receives inputs from real-world mobility data and integrates the route recommendations offered by leading navigation services’ APIs. Second, we use the framework to conduct controlled simulations in three cities. In our experiments, given a certain number of circulating vehicles, we vary the adoption rate of a navigation service. For each adoption rate, vehicles are randomly divided into treatment and control groups, with the treatment group following route recommendations and the control group not adhering to them.

We find that the aggregate impact of route recommendations is far from negligible. First, at high adoption rates and across all cities and navigation services, route diversity considerably decreases, i.e., vehicles are predominantly routed through fewer roads. This universal pattern amplifies the concentration of negative externalities such as congestion and emissions in specific city areas, making it difficult to control traffic concentration through public measures. Second, we delve into the relationship between adoption rate and CO<sub>2</sub> emissions. We discover that at low traffic loads – when a few vehicles traverse the city (e.g., off-peak hours) – navigation services consistently suggest optimal routes through an almost-empty road network, thereby reducing CO<sub>2</sub> emissions. However, at high traffic loads – when the traffic on the road network approaches congestion (e.g., peak hours) – the impact of navigation services depends on the

adoption rate. At a low adoption rate, the impact of navigation services is mainly beneficial and CO2 emissions decrease. However, once the penetration rate exceeds a service-specific threshold, these benefits diminish or even disappear. This underscores the existence of an “optimal” service adoption rate for each city, below which navigation services considerably reduce CO2 emissions compared to scenarios where adherence is absent. Finally, we discover that the relationship between the marginal shift in route diversity and the marginal shift of CO2 emissions can be effectively described by an exponential function. This enables us to forecast the marginal change in CO2 emissions as route diversity decreases, given the expansion of navigation service adoption throughout the population.

Our study provides an unprecedented view of the impact of navigation services on the urban environment. Our framework, which applies to any city provided the availability of mobility demand and road network data, may provide practical support for decision-makers to control the urban impact of digital platforms, implement strategies to reduce emissions, improve citizens’ well-being and design more sustainable cities.

## Simulation framework

We design a simulation framework to show how various navigation services affect urban traffic under various circumstances. This framework exploits SUMO, an open-source, state-of-the-art simulation tool for modelling urban traffic [29]. SUMO generates a lifelike representation of urban traffic based on a given road network and mobility demand (see Methods for details). The simulation can capture the behaviour of a set of vehicles, including their routes, traffic congestion, queues at traffic lights, and slowdowns due to heavy traffic, providing a realistic digital twin of vehicular traffic.

A city’s road network can be represented as a directed graph, where the set of nodes represents road intersections and the set of edges represents road edges (individual segments that connect road intersections). We use road networks made available on the public geographic information system OpenStreetMap (see Methods for details). We describe the mobility demand within the city as an origin-destination (OD) matrix  $M$ , where each element  $m_{o,d} \in M$  indicates the number of trips that start from location  $o$  and end at location  $d$ . An OD matrix may be obtained in various ways, such as through travel surveys, GPS traces, mobile phone data, or smart card transactions [20, 12, 36, 10]. In this study, we first divide the city into equally sized square tiles and leverage real-world GPS traces from thousands of private vehicles to compute the number of vehicles moving between any two tiles (see Methods for details). We then randomly select  $N$  trips, where each trip  $T_v = (e_o, e_d, t)$  is obtained by randomly selecting an element  $m_{o,d} \in M$  with probability  $p_{o,d} \propto m_{o,d}$ , uniformly selecting two road edges  $e_o, e_d$  within the corresponding tiles  $o$  and  $d$ , and uniformly selecting a starting time  $t$  during one hour. See Supplementary Note 1 for further details on the computation of the mobility demand.

We rely on public API-based navigation services to generate trip routes on the road network (see Methods for details). These services recommend a route between an origin  $o$  and a destination  $d$  considering various factors, such as the typical traffic conditions at the time  $t$  when the trip  $(o, d, t)$  starts. The trip  $(o, d, t)$  allows us to simulate drivers’ typical requests for these services, such as “Take me from location A to location B by car at 3:30 PM”. Note that navigation services also consider real-time traffic conditions in the real world when providing routes. These real-world conditions can be unpredictable due to exogenous factors (e.g., strikes, accidents, works in progress). To ensure consistency with our simulated traffic, we force the use of historical information making the request for a future time with respect to the time of the simulation. We consider a collection  $S$  of popular navigation services with public APIs, including Google Maps (GM), MapBox (MB), Bing Maps (Bi), TomTom fastest route (TTF), TomTom shortest route (TTS), and TomTom eco routing (EcoTT).<sup>1</sup> See Supplementary Note 2 for details. Figure 1a-b shows how different navigation services may provide different routes for the same trip. This variation arises because the services rely on different criteria and possess diverse historical data on traffic conditions. In general, we find that the average overlap between the routes provided by these services ranges from 70% to 97% (see Supplementary Note 2). Note that these algorithms are black boxes to us

---

<sup>1</sup>AppleMaps, Waze, and Google Maps eco-routing are unavailable due to the absence of public APIs.

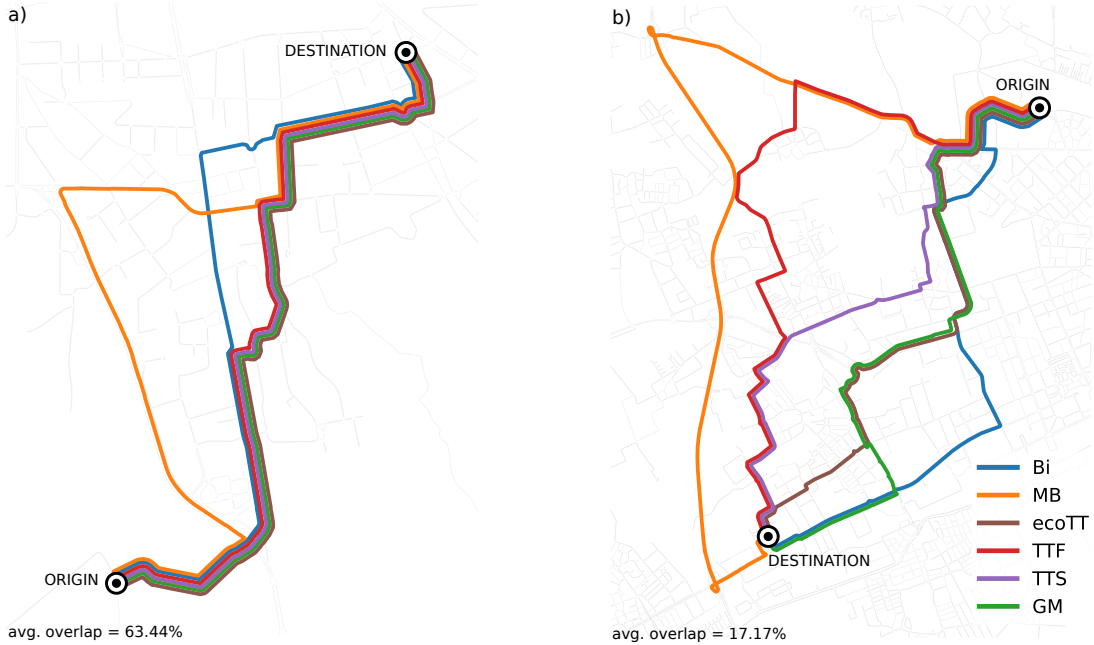


Figure 1: **Routes recommended by navigation services.** (a) Example of an origin-destination pair where suggestions by a navigation service (TTF) overlap considerably (63.44% on average). (b) Example where suggestions differ considerably (average overlap of 17.17%). Different navigation services generally suggest different routes for the same origin-destination pair. This variation occurs because the services rely on different criteria and possess diverse historical data on traffic conditions.

since the implementation specifics of these services are unknown. We refer to a trip that follows a route suggested by a navigation service  $s \in S$  as an  $s$ -routed trip.

To assess how a navigation service  $s \in S$  affects traffic in a given city, we design controlled experiments [34] varying the rate of adoption of  $s$  in the range  $r = 0\%, 10\%, 20\%, \dots, 100\%$ . Given  $r$ , we assign  $r\%$  of vehicles to a treatment group, and the remaining  $(100 - r)\%$  of vehicles to a control group. Vehicles in the treatment group are  $s$ -routed, while those in the control group follow a modified version of the fastest route on the road network recommended by SUMO<sup>2</sup>. This modification slightly lengthens the fastest route to account for the imperfections and irrational behaviour of human drivers [41] (see Methods and Supplementary Note 3). For statistical robustness, the simulation for a given adoption rate  $r$  is repeated ten times, each with a different random choice of the  $s$ -routed trips. Furthermore, we repeat all the above steps considering both low and high traffic loads. Low traffic loads refer to situations with few circulating vehicles in the city, such as off-peak hours and nighttime. High traffic load indicates that the traffic is approaching congestion, for example during peak hours. See Supplementary Note 4 for more details.

We evaluate the impact of navigation services in isolation, where all the vehicles in the simulation use the same service, and in combination, where vehicles may choose among different services (see Supplementary Note 5). We present only the isolation scenario because the results are analogous. To assess the urban impact of navigation services, we evaluate route diversity, i.e., the number of road edges traversed at least once by any vehicle, and the total CO<sub>2</sub> emissions produced by the vehicles. We compute the CO<sub>2</sub> emissions through a microscopic emission model [9] provided by SUMO that estimates the vehicle’s instantaneous emissions as a function of speed and acceleration (see Supplementary Note 6).

Our experimental setup has a main limitation that stems from interaction effects between vehicles on the road network [3]. The control group cannot be completely separated from the indirect effects of recommendations, as vehicles in the control group may encounter on the streets vehicles in the treatment group. Despite being a randomized controlled

<sup>2</sup><https://sumo.dlr.de/docs/duarouter.html>

simulation, our experiments do not satisfy the Stable Unit Treatment Value Assumption from causal inference [18]. As a result, we cannot provide unbiased estimates of causal quantities of interest, such as the average treatment effect. This is a common scenario when conducting controlled experiments in complex social systems, which also applies to social media platforms [23]. In this study, we present the results of different compositions of the treatment and the control group. Intuitively, we anticipate peer effects to reduce observable differences between the control and treatment groups. Therefore, our reported statistics likely underestimate the true causal effects of urban recommendations.

## Impact of navigation services

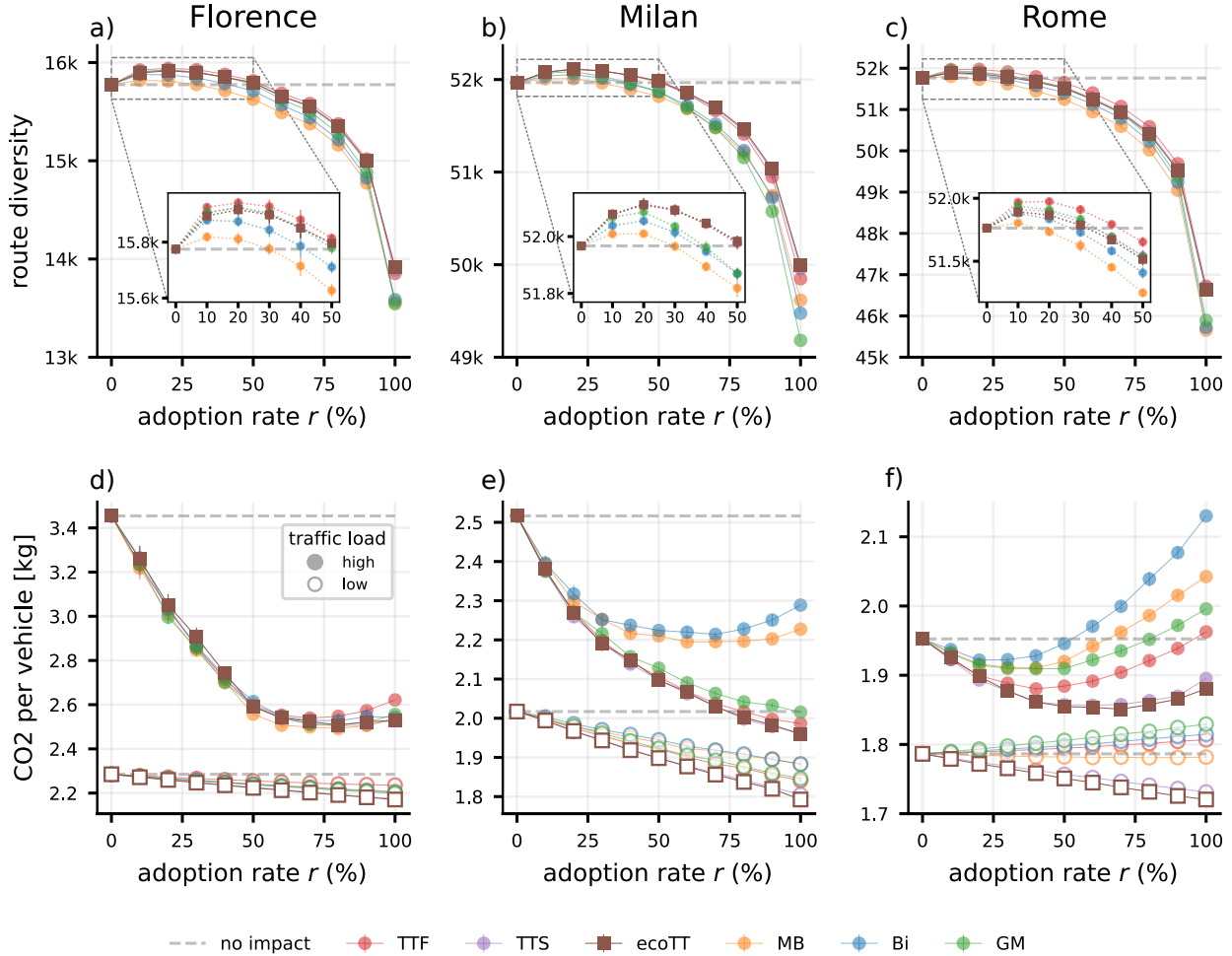
Our simulation framework can be applied to any city where data on the road network and mobility demand are available. We conduct experiments in three cities in Italy: Milan, Rome, and Florence. These cities were chosen due to the availability of GPS traces to compute the mobility demand and their heterogeneity in size, population, and road network structure, making them good candidates for testing the robustness of our simulation framework. For example, Rome is large but with the sparsest network; Milan is slightly smaller than Rome but with a denser network; Florence is small but with a dense road network (see Supplementary Table 1 for details on road networks).

Figure 2a-c illustrates the impact of varying the service adoption rate  $r$  on route diversity in the selected cities, considering high traffic loads. Results for low traffic loads are similar (see Supplementary Figure S1). If the navigation service had a negligible impact, we would expect a stable route diversity as  $r$  increases (dashed line in Figure 2a-c). Contrary to the assumption of insignificance, route diversity varies considerably with  $r$  following an exponential function (see Supplementary Note 7). When  $r$  is below a certain city- and service-dependent threshold ( $\approx 25$ -50%), route diversity slightly increases by 0.15-1.05% in Florence, 0.08-0.34% in Milan, and 0.01-0.41% in Rome (see inset plots in Figure 2a-c) compared to the no-impact scenario ( $r = 0\%$ ). On the other hand, when  $r$  exceeds this threshold, route diversity considerably decreases. At the total adoption rate ( $r = 100\%$ ), route diversity is considerably reduced by 11.80-14.34% in Florence, 3.79-6.87% in Milan, and 9.73-14.26% in Rome compared to the no-impact scenario. We also examine the distribution of route diversity separately for vehicles in the treatment and control groups at various adoption rates. We find that  $s$ -routed vehicles exhibit significantly lower route diversity compared to vehicles in the control group, regardless of the adoption rate (see Supplementary Note 8).

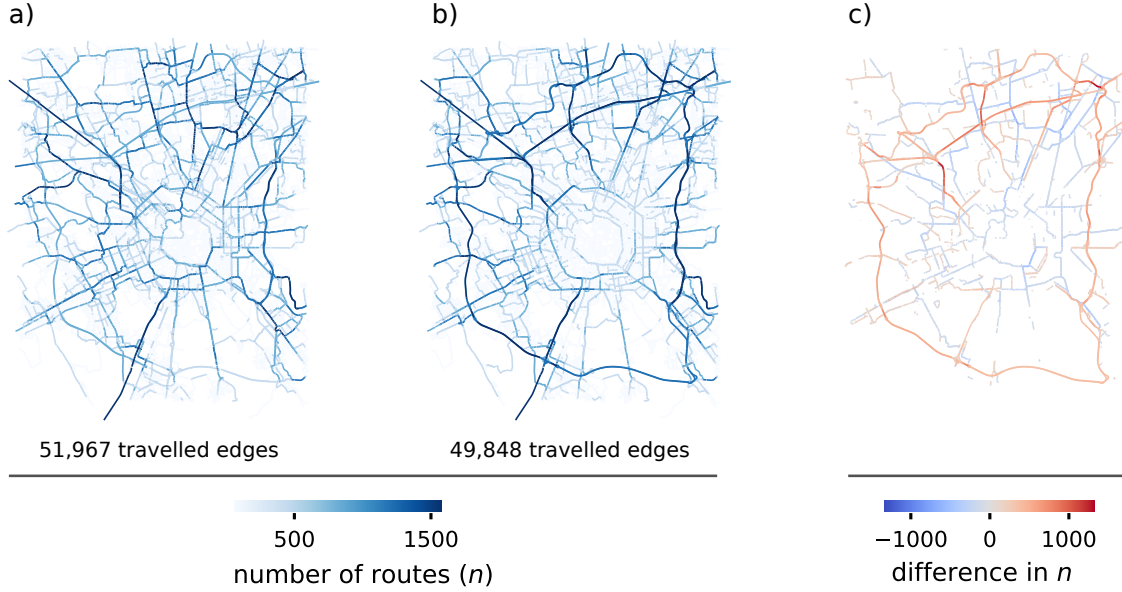
These results demonstrate that increased adoption of navigation services reduces route diversity, causing route conformity and leading to inefficient use of the road network. These trends are consistent under low and high traffic loads, with only minor fluctuations among navigation services. Route conformity emerges because navigation services tend to offer the same route to all vehicles with identical trips, leading to a concentration of traffic on fewer roads. This behaviour is exacerbated by the distribution of flows in the OD matrix, which shows that a small number of flows involve a large number of trips, while the majority involve fewer trips [6].

Figure 2d-f shows the average CO<sub>2</sub> emissions per vehicle produced at different adoption rates and traffic loads. When the traffic load is low, navigation services are generally beneficial. In most cases, CO<sub>2</sub> emissions are lower than they would be in the no-impact scenario (refer to Figure 2d-f), showing a near-linear decreasing trend with  $r$ . At the total adoption rate, navigation services can reduce CO<sub>2</sub> emissions by 2.15-5% in Florence and 6.64-11.13% in Milan. In Rome, some navigation services reduce CO<sub>2</sub> emissions by 0.26-3.69%, while GM, TTF and Bi slightly increase them by 2.4%, 1.13% and 1.57%, respectively.

At high traffic loads, the impact of navigation services depends on  $r$ . When  $r$  is low, CO<sub>2</sub> emissions decrease considerably; when  $r$  exceeds a certain city- and service-dependent threshold, the benefits plateau and in some cases CO<sub>2</sub> emissions even increase (see Figure 2d-f). Note that as the adoption rate reaches  $r = 100\%$  the overall CO<sub>2</sub> emissions become concentrated on a small fraction of routes due to the increased route conformity, thereby increasing the inequality of distribution of CO<sub>2</sub> emissions on roads (see Supplementary Note 9). Figure 3a-c illustrates this effect in Milan: at a 0% TTF adoption rate (Figure 3a), the traffic distribution is more even, whereas at a 100% adoption rate (3b), there is a concentration of traffic and CO<sub>2</sub> emissions on fewer roads. The use of navigation services also changes



**Figure 2: Impact of navigation services on route diversity and CO2 emissions.** (a-c) Service adoption rate ( $r$ ) versus route diversity at high traffic loads in Florence, Milan, and Rome. The dashed line represents the no-impact scenario ( $r=0\%$ ). Markers indicate the average route diversity over ten simulations with different random choices of  $s$ -routed vehicles. Squares refer to the navigation service ecoTT, which employs eco-routing. Vertical bars indicate the standard deviation. The inset plots zoom on the range  $r = 0\%, \dots, 50\%$ , where route diversity slightly increases. Increased adoption of navigation services reduces route diversity, with only minor fluctuations among navigation services. (d-f) Service adoption rate ( $r$ ) versus average CO2 emissions per vehicle at high (filled markers) and low (empty markers) traffic loads. The dashed line represents the no-impact scenario ( $r = 0\%$ ). Markers indicate the average CO2 emissions over ten simulations with different random choices of  $s$ -routed vehicles. Squares refer to ecoTT. Vertical bars indicate the standard deviation. At high traffic loads, when  $r$  is low, CO2 emissions decrease considerably; when  $r$  exceeds a certain city- and service-dependent threshold, the benefits plateau and, in some cases, even reverse.



**Figure 3: Road usage of navigation services.** (a, b) Route distribution of trips in Milan with TTF adoption rate  $r=0\%$  (a) and  $r=100\%$  (b). Darker edge colours indicate higher traffic concentration. When  $r=0\%$ , traffic is more spatially uniform than traffic when  $r=100\%$ , at which there is a concentration of routes on fewer edges. (c) Difference in road usage between  $r=100\%$  and  $r=0\%$ . Blue edges indicate where the total adoption of TTF reduces traffic compared to the scenario with no impact; red edges indicate where it concentrates traffic more.

the spatial distribution of routes across the road network of Milan, directing them towards highways and peripheral areas (Figure 3c). In Florence, the most effective adoption rate for all navigation services is around  $r = 70\text{-}80\%$ , resulting in an average CO2 reduction of about 27%; after this point, the benefits diminish (see Figure 3c). In Milan, GM and TomTom-based services (TTF, TTS, and ecoTT) consistently reduce CO2 emissions as  $r$  increase, achieving reductions of approximately 19-22% at the total adoption rate. In contrast, MB and Bi reach their highest reductions ( $\approx 12\%$ ) when  $r = 60\%$  and  $r = 70\%$ , respectively; beyond these rates, the benefits considerably diminish (CO2 reductions decrease by 9%). In Rome, optimal adoption rates vary by service: 20% for Bi, 40% for MB, GM and TTF, 60% for TTS, and 70% for ecoTT, leading to an average CO2 reduction of 3.29%. Notably, Bi, MB, GM and TTF in Rome lead to increased CO2 emissions beyond certain thresholds compared to the baseline scenario: 9.10% for Bi, 4.61% for MB, 2.22% for GM and 0.52% for TTF (see Supplementary Table 2 for details on the CO2 reductions).

Our simulations reveal that even an eco-routing service (EcoTT) shows CO2 trends similar to the other navigation services (see Figure 2). This suggests that relying solely on eco-routing is inadequate for fully controlling the impact of algorithmic urban recommendations. Being eco-friendly is not just a property of an individual route but also of drivers' aggregate behaviour.

We also explore the relationship between route diversity and total CO2 emissions during periods of high traffic load by examining the correlation between  $\Delta D_r$  and  $\Delta E_r$ . Here,  $\Delta D_r$  represents the marginal change in route diversity, while  $\Delta E_r$  denotes the marginal change in CO2 emissions (for more details, see Methods). We compute  $\Delta D_r$  as the difference in route diversity values between adoption rates  $r - 10\%$  and  $r$ . Similarly,  $\Delta E_r$  is the difference in CO2 emissions over the same interval. A positive  $\Delta E_r$  indicates a decrease of CO2 emissions at adoption rate  $r$  compared to  $r - 10\%$ , whereas a positive  $\Delta D_r$  indicates a decrease of route diversity at  $r$  compared to  $r - 10\%$ .

Our analysis reveals a non-linear correlation between  $\Delta D_r$  and  $\Delta E_r$  for all cities and navigation services. In Florence, Spearman's rank correlation coefficient is  $\rho = -0.958$ ; in Milan, it is  $\rho = -0.882$ , and in Rome, it is  $\rho = -0.899$ . This relationship is well described by an exponential decay function:  $\Delta E_r = \alpha e^{-\beta \Delta C_r} + \gamma$ . In this formula, the coefficient

$\beta$  measures how quickly incremental CO2 changes ( $\Delta E_r$ ) respond to incremental changes in route diversity ( $\Delta D_r$ ). A higher  $\beta$  indicates a more rapid CO2 change per unit change in route diversity. Milan has the highest coefficient value ( $\beta = 0.0068$ ), indicating that changes in route diversity have a more significant impact on CO2 reduction compared to Florence ( $\beta = 0.00313$ ) and Rome ( $\beta = 0.00226$ ).

Figure 4 illustrates this trend. At low adoption rates, slight increases in route diversity (i.e., a negative  $\Delta D_r$ , highlighted in grey) lead to substantial reductions in CO2 emissions. As  $r$  increases, small reductions in route diversity result in moderate CO2 reductions. However, as  $\Delta D_r$  further increases,  $\Delta E_r$  decreases, indicating a diminishing return effect. This pattern is consistent across all cities and navigation services (Figure 4d-f), suggesting that while initial efforts to optimize routes are highly effective, their efficiency decreases as further reductions in route diversity yield progressively smaller CO2 reduction benefits. Therefore, the positive impact of navigation services on reducing CO2 emissions diminishes as route diversity decreases.

We also investigate how the relationship between  $\Delta D_r$  and  $\Delta E_r$  is affected by the number  $N$  of circulating vehicles. We find that the exponential relationship stabilizes when the number of vehicles is greater than or equal to a certain city-dependent threshold (see Supplementary Note 10).

## Discussion

While navigation services may be beneficial under certain conditions, they significantly alter traffic patterns, environmental quality, and social equity within urban ecosystems. In all cities examined, navigation services substantially impact urban mobility, with a consistent pattern emerging: as the adoption rate increases, traffic and emissions become concentrated on fewer roads due to increased route conformity. This exacerbates exposure inequality, as the navigation services reshape the neighbourhoods in ways that can disproportionately burden certain areas with traffic and emissions. Furthermore, navigation services can interfere with existing routing policies, undermining local strategies designed to enhance safety and distribute traffic evenly or differently, such as routing traffic away from schools or hospitals. The example of Leonia exemplifies an extreme case of how navigation services can disrupt local traffic patterns. Additionally, rerouting traffic can impact the economic and social fabric of neighbourhoods. Areas with increased traffic may experience a decline in property values and overall urban equity issues. Conversely, areas bypassed by traffic might suffer reduced business activity as potential customers are diverted elsewhere. Our simulation framework has the potential to become a powerful what-if tool for urban policymakers with the aim of estimating the intensity and the localization of the concentration effect of navigation services and designing mitigating interventions.

Our study can be easily reproduced in any city, as it only requires widely available data on the city’s mobility demand and road network, as well as publicly accessible navigation services’ APIs. Upcoming legislation, such as the EU’s Digital Services Act and Digital Market Act, mandates the introduction of transparency measures on the algorithms used by very large online platforms, including navigation services, for recommending content or products to users. In this regard, our study marks an initial stride towards systematically assessing algorithmic influence on urban ecosystems and a conceptual and methodological foundation for agile responses to collective goal challenges.

The core emergent pattern underlying the impact of navigation services is route conformity, which erodes diversity in driver behaviour, leading to inefficient road network utilization and concentration of negative externalities. Our results corroborate recent research showing that promoting route diversity among drivers may have several benefits for traffic flow, including reducing CO2 emissions [17, 34]. Future research should further explore the balance between conformity and diversity, and develop strategies to inject diversity into routing behaviour when traffic load and the adoption rate of navigation services are high [38, 35].

This study opens avenues for further exploration. For instance, investigating navigation services’ effects on additional externalities like accident rates and pedestrian safety could provide deeper insights. Additionally, applying our framework to other mobility services presents an intriguing prospect. Similarly to navigation services, the collective

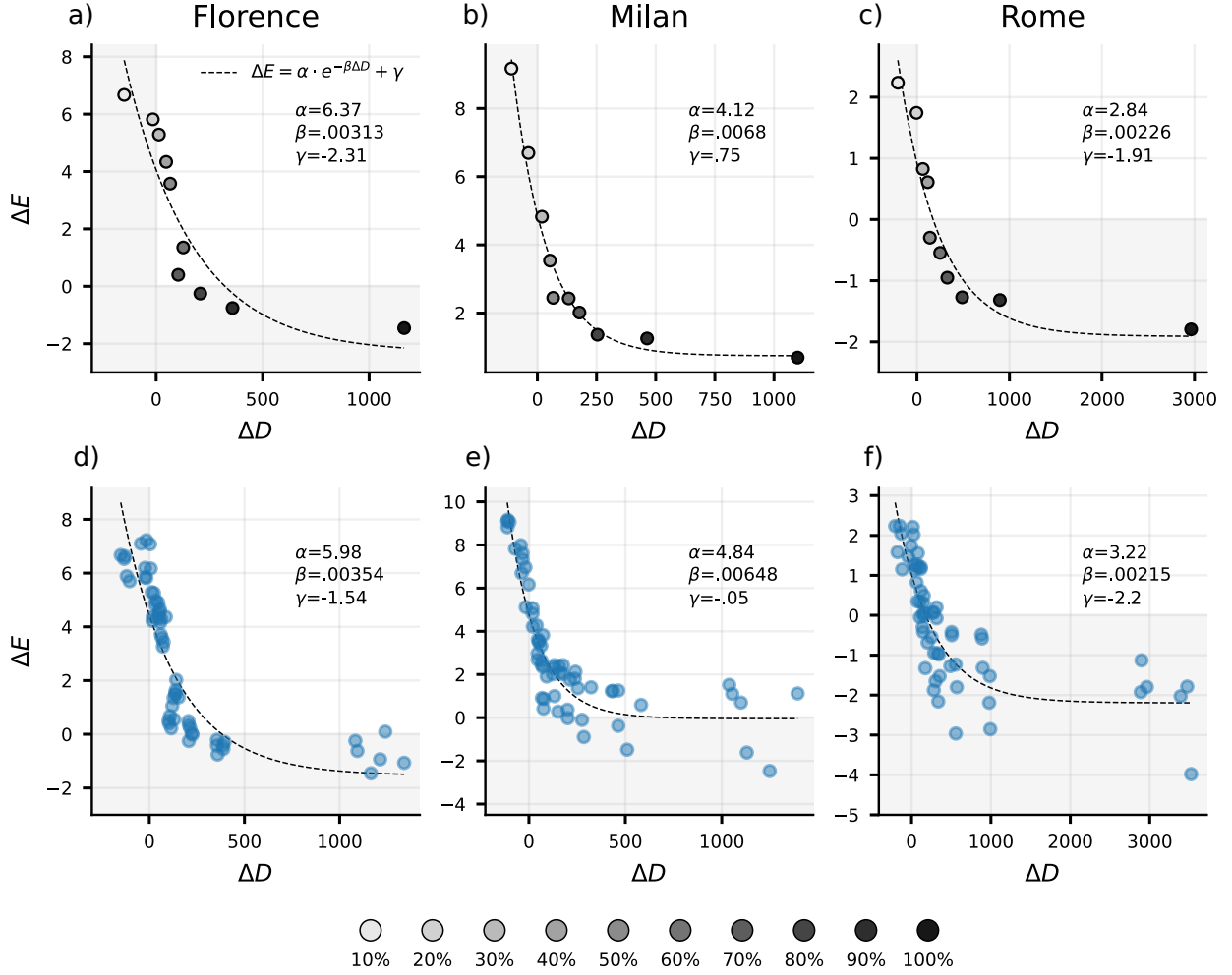


**Figure 4: Relationship between route diversity and CO<sub>2</sub> emissions.** (a-c) The relationship between the marginal change in route diversity ( $\Delta D_r$ ) and the marginal change in CO<sub>2</sub> emissions ( $\Delta E_r$ ) for TTF in Florence, Milan, and Rome. We find similar results for the other navigation services. The points are shaded from light grey to black, representing the service adoption rate (from  $r=10\%$  to  $r=100\%$ ). (d-f) The relationship between  $\Delta D_r$  and  $\Delta E_r$  for all navigation services. Regions where  $\Delta D_r$  or  $\Delta E_r$  are negative are highlighted in grey. The black dashed line represents the exponential decay fit for each scenario. At low adoption rates, slight increases in route diversity lead to substantial reductions in CO<sub>2</sub> emissions. As  $r$  increases, small reductions in route diversity result in moderate CO<sub>2</sub> reductions. However, as  $\Delta D_r$  further increases,  $\Delta E_r$  decreases, indicating a diminishing return effect. This pattern is consistent across all cities and navigation services.

impact of car-sharing and ride-hailing remains ambiguous: for example, recent evidence indicates that these services might worsen traffic congestion and emissions, undermining public transport while also raising equity concerns [34, 33, 48]. Our adaptable framework can help both assess these services’ evolving impact and validate strategies to mitigate their unintended consequences, whether through individualistic or cooperative approaches.

Meanwhile, our study has the potential to shape the emerging discussion around human-AI coevolution [38], particularly in terms of how we can measure and understand the intertwined influence between humans and recommenders in human-AI ecosystems. The dynamic interaction between drivers and navigation services creates a feedback loop: travel times, which influence recommendations, are shaped by drivers’ route choices, which have in turn been influenced by previous recommendations. As a consequence, drivers’ behaviour may then alter travel times, influencing subsequent recommendations. Our study has revealed a significant relationship between adoption rate of the service, route diversity and CO<sub>2</sub> emissions. The next step involves understanding how this relationship evolves in time within the human-recommender feedback loop.

By understanding and managing the relationship between drivers and navigation services, we have the potential to anticipate the level of emissions in our urban environments and take immediate, informed actions when they overcome a certain tolerance threshold. This is crucial because the decisions made by policymakers rely on the accuracy of our measurements and the promptness of our response to these measurements.

## Methods

**Road Networks.** A city’s road network is modelled as a directed weighted multigraph  $G = (V, E)$ , where  $V$  denotes the set of nodes representing intersections, and  $E$  is a multiset of edges representing the road segments connecting the vertices. Each edge  $e_{i,j} \in E$ , with  $i, j \in V$ , is associated with its minimum expected travel time  $t(e_{i,j})$ , capacity  $c(e_{i,j})$ , and speed limit  $s(e_{i,j})$ .

We extracted the road networks using OSM Web Wizard, which retrieves and pre-process road network data from OpenStreetMap (OSM). Following the approach described in [2], we manually fine-tune the road networks to correct inaccuracies that could potentially cause deadlocks and other unrealistic behaviours, thus negatively impacting the simulations. This fine-tuning phase includes correcting lane number inaccuracies, addressing road continuity disruptions, and modifying turns to align with real-world conditions. We use Google Maps and StreetView as benchmarks to ensure the accuracy of these adjustments.

**Traffic simulator.** SUMO (Simulation of Urban MObility) is an open-source agent-based traffic simulator allowing intermodal traffic simulation, including road vehicles, public transport, and pedestrians [29]. It simulates each vehicle’s dynamics, considering interactions with other vehicles, traffic jams, queues at traffic lights, and slowdowns caused by heavy traffic, supporting various route choice methods and routing strategies [2].

To simulate a traffic scenario, SUMO requires two primary input elements: a road network and a traffic demand. The road network describes the virtual road infrastructure where simulated vehicles move during the simulation. The traffic demand outlines the vehicles’ movement on the road network. We describe a vehicle’s movements as a route, i.e., a sequence of interconnected edges linking an origin to a destination and a departure time.

SUMO can simulate vehicular pollutant emissions utilizing the HBEFA3 emission model derived from the Handbook of Emission Factors for Road Transport (HBEFA) database [27]. The HBEFA3-based model estimates the vehicle’s instantaneous CO<sub>2</sub> emissions relying on the following function, which is linked to the power the vehicle’s engine produces in each trajectory point  $j$  to overcome the driving resistance force [27]:

$$\mathcal{E}(j) = c_0 + c_1 sa + c_2 sa^2 + c_3 s + c_4 s^2 + c_5 s^3$$

	provider	profile name	profile description	url
Bi	Bing Maps	timeWithTraffic	optimization of travel time using current traffic information.	bit.ly/ref_b
MB	Mapbox	driving-traffic	lowest probability of slowdowns given current and historical traffic conditions.	bit.ly/ref_mb
ecoTT	TomTom	eco	trade-off between travel time and fuel consumption	bit.ly/ref_tt
TTF	TomTom	fastest	shortest travel time while keeping the routes sensible.	bit.ly/ref_tt
TTS	TomTom	short	trade-off between travel time and travel distance.	bit.ly/ref_tt
GM	Google Maps	not available	not available	bit.ly/ref_gm

Table 1: Characteristics of navigation services’ APIs: service provider, routing criteria (profile name), description of the routing strategy, and URL with the documentation.

where  $s$  and  $a$  are the vehicle’s speed and acceleration in point  $j$ , respectively, and  $c_0, \dots, c_5$  are parameters specific to each emission type and vehicle taken from the HBEFA database. In this work we use SUMO version 1.19.0.

**Navigation services APIs.** Vehicles in the treatment group follow routes suggested by various navigation services. We utilized a collection of widely-used navigation services with publicly accessible APIs, including Bing Maps (Bi), MapBox (MB), TomTom eco routing (EcoTT), TomTom fastest route (TTF), and TomTom short (TTS). These services provided routes between an origin and a destination at a specified departure time, considering various factors such as typical traffic conditions at the time of departure. The rationale behind selecting these specific navigation services is based on their popularity, availability of public APIs, and variety in routing criteria, which provide a broad perspective on route suggestions. Additionally, these services cover many routing preferences, from eco-friendly to the fastest and shortest routes, offering a comprehensive comparison. Table 1 presents a detailed overview of the key characteristics of each navigation service, including the service name, service provider, whether it accounts for historical traffic, the name of the profile used (i.e., the routing criteria), a description, and the URL of the reference documentation.

As the route recommendations from the APIs are typically provided as sequences of GPS points, we employed a map-matching procedure to integrate these routes into the SUMO simulator. Specifically, we applied the state-of-the-art Longest Common Subsequence (LCSS) algorithm [50] to convert the sequence of GPS points into a sequence of connected edges in the SUMO road network, accurately representing the suggested routes.

**Modified fastest route.** Vehicles in the control group follow a modified version of the fastest route implemented by SUMO’s duarouter algorithm.<sup>3</sup> Duarouter is a valuable tool for simulating human driving and routing behaviour. It computes vehicle routes with an adjustable degree of variability, controlled by a parameter  $w \in [1, +\infty)$ . When  $w = 1$ , duarouter calculates the standard fastest route on the road network. When  $w > 1$ , it dynamically alters the edge weights (expected travel time) by a random factor uniformly drawn from the interval  $[1, w)$ . This random process ensures that different vehicles may get different routes even if their trip has the same origin and destination. As  $w$  increases, the extent of randomness in the route calculation also increases, resulting in routes that can diverge significantly from the fastest route (see Supplementary Information 3). This increased route variability helps us model the imperfections of human driving behaviour, which often deviates from the fastest route due to personal preferences, lack of complete knowledge of the road network, and irrational behaviours [41, 51].

**GPS Data.** To estimate each city’s mobility demand, we use a vehicular GPS trajectory dataset provided by OCTO, a company that provides a data collection service for insurance companies. This dataset describes the trajectories of thousands of vehicles for various Italian localities over an entire year. While the market penetration of the dataset varies, it generally represents a minimum of 2% of the total registered vehicles. Our analysis focuses on the cities of Florence, Milan, and Rome, selected due to the availability of GPS traces suitable for computing origin-destination

<sup>3</sup><https://sumo.dlr.de/docs/duarouter.html>

(OD) matrices, their diverse sizes, populations, and road network structures. The raw dataset includes 7,102,351 GPS points from 24,640 vehicles in Florence, 143,698,720 GPS points from 106,456 vehicles in Milan, and 26,801,872 GPS points from 30,763 vehicles in Rome.

The dataset’s validity and reliability are corroborated by its extensive use in prior studies [8, 37, 9]. We processed the raw GPS dataset to create segmented trajectories that represent semantic journeys as follows:

- We eliminate noise by filtering out GPS points with speeds exceeding 250 km/h [49];
- We use a stop detection algorithm [49] to segment each trajectory into sub-trajectories based on identified stops. A stop is identified when a vehicle remains within a distance of 0.2 km from a trajectory point for at least 20 minutes;
- We considered only trips that both start and end within the predefined area of interest. For trips that start or end outside this area but traverse it, we used the first entry point within the area as the origin and the last exit point as the destination. This method preserves commuter trips originating or ending outside the city.

To compute the OD matrix reflecting a city’s traffic patterns, we first discretize the city into 1 km<sup>2</sup> squared tiles using scikit-mobility [36]. We then extract flows from the pre-processed segmented trajectories to fit the OD matrix.

We compute the flows by considering only trips with a duration between 5 and 60 minutes that depart during the morning peak hours on all Wednesdays. Focusing on morning peak hours allows us to model high-traffic scenarios, as they represent periods of intense traffic congestion. By selecting Wednesdays, we ensure the capture of typical weekday traffic, avoiding anomalies associated with weekends or specific weekdays with unique traffic patterns. We exclude outlier weeks (e.g., holidays) from the analysis. Additionally, we filter out infrequent flows, retaining only those that occur regularly. See [Supplementary Note 1](#) for further details on the pre-processing and flow computation.

After the preprocessing step, the dataset used to compute the OD matrix includes 5,477 trips from 1,184 vehicles for Florence (616 distinct flows); 113,323 trips from 15,997 vehicles for Milan (11,967 distinct flows); and 13,647 trips from 1,965 vehicles for Rome (1,757 distinct flows).

For each city, based on the pre-processed data, we obtain an origin-destination matrix  $M$ , where an element  $m_{o,d} \in M$  denotes the number of trips that start in tile  $o$  and end in tile  $d$ . Each vehicle’s trip starting and ending tiles determine the origins and destinations.

**Data and Code availability.** The processed road networks for Florence, Milan, and Rome utilized in this study are accessible at <https://github.com/GiulianoCornacchia/Urban-Impact-Navigators>. The OCTO dataset used in our research is proprietary and thus not publicly available. Consequently, we cannot provide the original OD matrices derived from this dataset. To overcome this limitation, we have provided the necessary code to generate an OD matrix for Milan utilizing a publicly accessible dataset available at [https://ckan-sobigdata.d4science.org/dataset/gps\\_track\\_milan\\_italy](https://ckan-sobigdata.d4science.org/dataset/gps_track_milan_italy). Additionally, we provide a routine to create random OD matrices, which can be helpful in scenarios where trajectory data is unavailable.

Due to proprietary restrictions, the specific navigation service suggestions used in our study cannot be included. However, we have included code to generate the fastest route, replicating the functionality of a navigation service prototype. This code also includes routines to generate perturbations of the fastest routes for non-routed vehicles.

The Python code for replicating the analyses in the study is publicly available at <https://github.com/GiulianoCornacchia/Urban-Impact-Navigators>.

**Acknowledgements.** This work has been partially supported by: EU project H2020 SoBigData++ G.A. 871042; PNRR (Piano Nazionale di Ripresa e Resilienza) in the context of the research program 20224CZ5X4 PE6 PRIN 2022 “URBAI – Urban Artificial Intelligence” (CUP B53D23012770006), funded by the European Commission under the

Next Generation EU programme; and by PNRR - M4C2 - Investimento 1.3, Partenariato Esteso PE00000013 - "FAIR – Future Artificial Intelligence Research" – Spoke 1 "Human-centered AI", funded by the European Commission under the NextGeneration EU programme. We thank Daniele Fadda for his precious support with data visualization.

**Author contributions** GC conceptualized the work, developed the simulation framework, performed the experiments, made the plot and wrote the paper. LP conceptualized the work, designed the experiments, wrote the paper, and supervised the research. MN conceptualized the work. DP conceptualized the work and wrote the paper. All authors read and approved the paper.

**Corresponding authors** The corresponding authors are G.C. (giuliano.cornacchia@phd.unipi.it) and L.P. (luca.pappalardo@isti.cnr.it)

## References

- [1] K. Ahn and H. A. Rakha. Network-wide impacts of eco-routing strategies: A large-scale case study. *Transportation Research Part D: Transport and Environment*, 25:119–130, 2013.
- [2] J. Argota Sánchez-Vaquerizo. Getting real: The challenge of building and validating a large-scale digital twin of barcelona’s traffic with empirical data. *ISPRS International Journal of Geo-Information*, 11(1), 2022.
- [3] P. M. Aronow and C. Samii. Estimating average causal effects under general interference, with application to a social network experiment. *The Annals of Applied Statistics*, 11(4):1912–1947, 2017.
- [4] N. Arora, T. Cabannes, S. Ganapathy, Y. Li, P. McAfee, M. Nunkesser, C. Osorio, A. Tomkins, and I. Tsogsuren. Quantifying the sustainability impact of google maps: A case study of salt lake city. Oct. 2021.
- [5] E. Bakshy, S. Messing, and L. A. Adamic. Exposure to ideologically diverse news and opinion on facebook. *Science*, 348(6239):1130–1132, 2015.
- [6] H. Barbosa, M. Barthelemy, G. Ghoshal, C. R. James, M. Lenormand, T. Louail, R. Menezes, J. J. Ramasco, F. Simini, and M. Tomasini. Human mobility: Models and applications. *Physics Reports*, 734:1–74, 2018.
- [7] M. Barth, K. Boriboonsomsin, and A. Vu. Environmentally-friendly navigation. In *2007 IEEE Intelligent Transportation Systems Conference*, pages 684–689, 2007.
- [8] A. Bazzani, B. Giorgini, R. Gallotti, L. Giovannini, M. Marchioni, and S. Rambaldi. Towards congestion detection in transportation networks using gps data. In *2011 IEEE Third International Conference on Privacy, Security, Risk and Trust and 2011 IEEE Third International Conference on Social Computing*, pages 1455–1459. IEEE, 2011.
- [9] M. Böhm, M. Nanni, and L. Pappalardo. Gross polluters and vehicle emissions reduction. *Nature Sustainability*, pages 1–9, June 2022.
- [10] P. Bonnel, M. Fekih, and Z. Smoreda. Origin-destination estimation using mobile network probe data. *Transportation Research Procedia*, 32:69–81, 2018.
- [11] P. J. Brantingham. The logic of data bias and its impact on place-based predictive policing. *Ohio State Journal of Criminal Law*, 2017.
- [12] S. Cerqueira, E. Arsenio, and R. Henriques. Inference of dynamic origin–destination matrices with trip and transfer status from individual smart card data. *European Transport Research Review*, 14(1):1–18, 2022.
- [13] W. Chen, D. Pacheco, K.-C. Yang, and F. Menczer. Neutral bots probe political bias on social media. *Nature communications*, 12(1):5580, 2021.
- [14] D. Cheng, O. Gkountouna, A. Züfle, D. Pfoser, and C. Wenk. Shortest-path diversification through network penalization: A washington dc area case study. In *Proceedings of the 12th ACM SIGSPATIAL International*

*Workshop on Computational Transportation Science, IWCTS'19*, New York, NY, USA, 2019. Association for Computing Machinery.

- [15] M. Cinelli, G. De Francisci Morales, A. Galeazzi, W. Quattrociocchi, and M. Starnini. The echo chamber effect on social media. *Proceedings of the National Academy of Sciences*, 118(9):e2023301118, 2021.
- [16] G. Cornacchia, M. Böhm, G. Mauro, M. Nanni, D. Pedreschi, and L. Pappalardo. How routing strategies impact urban emissions. In *Proceedings of the 30th International Conference on Advances in Geographic Information Systems*, pages 1–4, 2022.
- [17] G. Cornacchia, M. Nanni, and L. Pappalardo. One-shot traffic assignment with forward-looking penalization. In *Proceedings of the 31st ACM International Conference on Advances in Geographic Information Systems*, pages 1–10, 2023.
- [18] D. R. Cox. *Planning of experiments*. 1958.
- [19] L. W. Foderaro. Navigation apps are turning quiet neighborhoods into traffic nightmares. *The New York Times*.
- [20] M. L. Hazelton. Inference for origin–destination matrices: estimation, prediction and reconstruction. *Transportation Research Part B: Methodological*, 35(7):667–676, 2001.
- [21] S. Hendrix. Traffic-weary homeowners and waze are at war, again. guess who’s winning. *The Washington Post*, 2016.
- [22] B. Howe, J. M. Brown, B. Han, B. Herman, N. Weber, A. Yan, S. Yang, and Y. Yang. Integrative urban AI to expand coverage, access, and equity of urban data. *The European Physical Journal Special Topics*, 231(9):1741–1752, 2022.
- [23] F. Huszár, S. I. Ktena, C. O’Brien, L. Belli, A. Schlaikjer, and M. Hardt. Algorithmic amplification of politics on twitter. *Proceedings of the National Academy of Sciences*, 119(1), Jan. 2022.
- [24] INFRAS. Handbuch für emissionsfaktoren. <http://www.hbefa.net/>, 2013.
- [25] I. Johnson, J. Henderson, C. Perry, J. Schöning, and B. Hecht. Beautiful... but at what cost? an examination of externalities in geographic vehicle routing. *Proc. ACM Interact. Mob. Wearable Ubiquitous Technol.*, 1(2), jun 2017.
- [26] J. Kleinberg, J. Ludwig, S. Mullainathan, and C. R. Sunstein. Algorithms as discrimination detectors. *Proceedings of the National Academy of Sciences*, 117(48):30096–30100, Dec. 2020.
- [27] D. Krajzewicz, M. Behrisch, P. Wagner, R. Luz, and M. Krumnow. Second generation of pollutant emission models for sumo. In M. Behrisch and M. Weber, editors, *Modeling Mobility with Open Data*, pages 203–221, Cham, 2015. Springer International Publishing.
- [28] D. Lee and K. Hosanagar. How do recommender systems affect sales diversity? a cross-category investigation via randomized field experiment. *Information Systems Research*, 30(1):239–259, 2019.
- [29] P. A. Lopez, M. Behrisch, L. Bieker-Walz, J. Erdmann, Y.-P. Flötteröd, R. Hilbrich, L. Lücken, J. Rummel, P. Wagner, and E. Wiessner. Microscopic traffic simulation using sumo. In *2018 21st International Conference on Intelligent Transportation Systems (ITSC)*, pages 2575–2582, 2018.
- [30] J. Macfarlane. Your navigation app is making traffic unmanageable. *IEEE Spectrum*, pages 22–27.
- [31] M. McCarty. The road less traveled? not since waze came to los angeles. *NPR All Tech Considered*, 2016.
- [32] N. Mehrabi, F. Morstatter, N. Saxena, K. Lerman, and A. Galstyan. A survey on bias and fairness in machine learning. *ACM Computing Surveys*, 54(6):1–35, 2021.
- [33] N. S. Ngo, T. Götschi, and B. Y. Clark. The effects of ride-hailing services on bus ridership in a medium-sized urban area using micro-level data: Evidence from the lane transit district. *Transport Policy*, 105:44–53, 2021.

- [34] L. Pappalardo, E. Ferragina, S. Citraro, G. Cornacchia, M. Nanni, G. Rossetti, G. Gezici, F. Giannotti, M. Lalli, D. Gambetta, et al. A survey on the impact of ai-based recommenders on human behaviours: methodologies, outcomes and future directions. *arXiv preprint arXiv:2407.01630*, 2024.
- [35] L. Pappalardo, E. Manley, V. Sekara, and L. Alessandretti. Future directions in human mobility science. *Nature Computational Science*, 2023.
- [36] L. Pappalardo, F. Simini, G. Barlacchi, and R. Pellungrini. scikit-mobility: A Python Library for the Analysis, Generation, and Risk Assessment of Mobility Data. *Journal of Statistical Software*, 103(4):1–38, 2022.
- [37] L. Pappalardo, F. Simini, S. Rinzivillo, D. Pedreschi, F. Giannotti, and A.-L. Barabási. Returners and explorers dichotomy in human mobility. *Nature Communications*, 6:8166, Sept. 2015.
- [38] D. Pedreschi, L. Pappalardo, E. Ferragina, R. Baeza-Yates, A.-L. Barabasi, F. Dignum, V. Dignum, T. Eliassi-Rad, F. Giannotti, J. Kertesz, A. Knott, Y. Ioannidis, P. Lukowicz, A. Passarella, A. S. Pentland, J. Shawe-Taylor, and A. Vespignani. Human-ai coevolution, 2024.
- [39] F. Perez-Prada, A. Monzón, and C. Valdés. Managing traffic flows for cleaner cities: The role of green navigation systems. *Energies*, 10:791, 06 2017.
- [40] N. Perra and L. E. C. Rocha. Modelling opinion dynamics in the age of algorithmic personalisation. *Scientific Reports*, 9(1):7261, May 2019.
- [41] S. Seele, T. Dettmar, R. Herpers, C. Bauckhage, and P. Becker. Cognitive aspects of traffic simulations in virtual environments. *SNE Simul. Notes Eur.*, 22(2), 2012.
- [42] A. Sîrbu, D. Pedreschi, F. Giannotti, and J. Kertész. Algorithmic bias amplifies opinion fragmentation and polarization: A bounded confidence model. *PLOS ONE*, 14(3):e0213246, 2019.
- [43] S. Siuhi and J. Mwakalonge. Opportunities and challenges of smart mobile applications in transportation. *Journal of Traffic and Transportation Engineering*, 3(6):582–592, 2016.
- [44] J. Thai, N. Laurent-Brouty, and A. M. Bayen. Negative externalities of gps-enabled routing applications: A game theoretical approach. In *2016 IEEE 19th International Conference on Intelligent Transportation Systems (ITSC)*, pages 595–601, 2016.
- [45] C. Valdes, F. Perez-Prada, and A. Monzon. Eco-routing: More green drivers means more benefits. In *Proceedings of the XII Conference on Transport Engineering, Valencia, Spain*, pages 7–9, 2016.
- [46] C. Wagner, M. Strohmaier, A. Olteanu, E. Kiciman, N. Contractor, and T. Eliassi-Rad. Measuring algorithmically infused societies. *Nature*, 595(7866):197–204, July 2021.
- [47] I. Waller and A. Anderson. Quantifying social organization and political polarization in online platforms. *Nature*, 600(7888):264–268, 2021.
- [48] A. Yan and B. Howe. Fairness-Aware demand prediction for new mobility. In *Proceedings of the AAAI Conference on Artificial Intelligence*, volume 34, pages 1079–1087, 2020.
- [49] Y. Zheng. Trajectory data mining: An overview. *ACM Trans. Intell. Syst. Technol.*, 6(3), may 2015.
- [50] L. Zhu, J. R. Holden, and J. D. Gonder. Trajectory segmentation map-matching approach for large-scale, high-resolution gps data. *Transportation Research Record*, 2645(1):67–75, 2017.
- [51] S. Zhu and D. Levinson. Do people use the shortest path? an empirical test of wardrop’s first principle. *PLOS ONE*, 10(8):1–18, 08 2015.

# Supplementary Material

## A Supplementary Figures

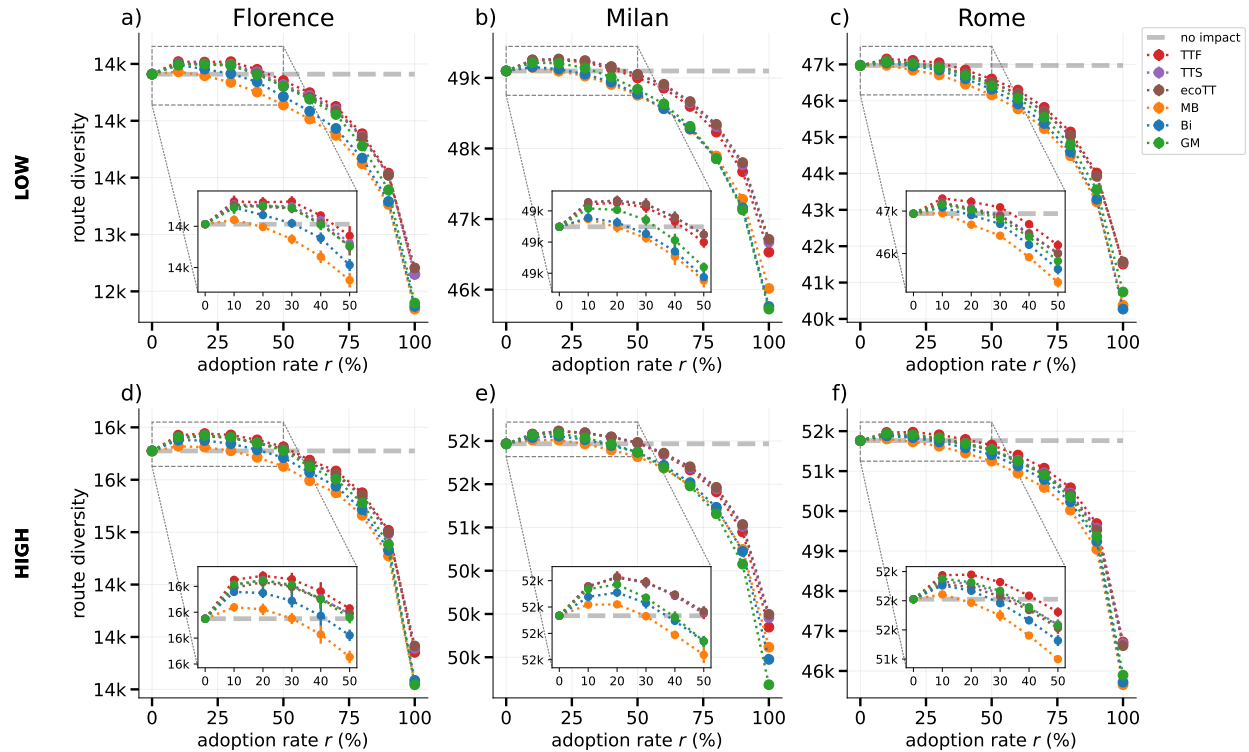


Figure S1: Service adoption rate versus route diversity at low (a-c) and high (d-f) traffic loads in Florence, Milan, and Rome. The dashed line represents the no-impact scenario (adoption rate  $r = 0\%$ ). In the error bars, points indicate the average route diversity over ten simulations with different choices of  $s$ -routed vehicles chosen uniformly at random. Vertical bars indicate the standard deviation. The inset plots zoom on the range  $r = 0\%, \dots, 50\%$ , where route diversity slightly increases. The consistency of this universal pattern is evident across different cities and varying traffic conditions.

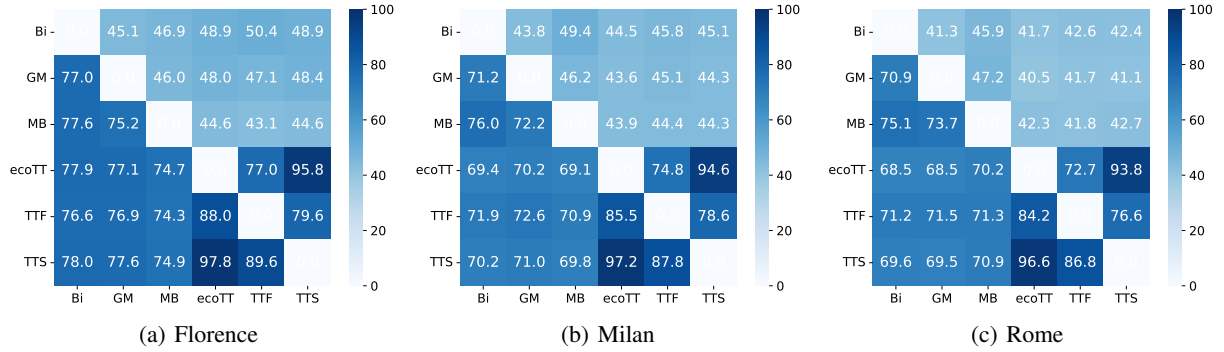


Figure S2: Average overlap (below the diagonal) and the percentage of exact matches (above the diagonal) of routes suggested by different navigation services for the same trips in three cities: (a) Florence, (b) Milan, and (c) Rome. For each cell below the diagonal, the value represents the average overlap computed for each route pair between two services. The services compared include Bi, MB, GN, ecoTT, TTF, and TTS. The color intensity represents the value, with darker shades indicating higher percentages and overlaps.

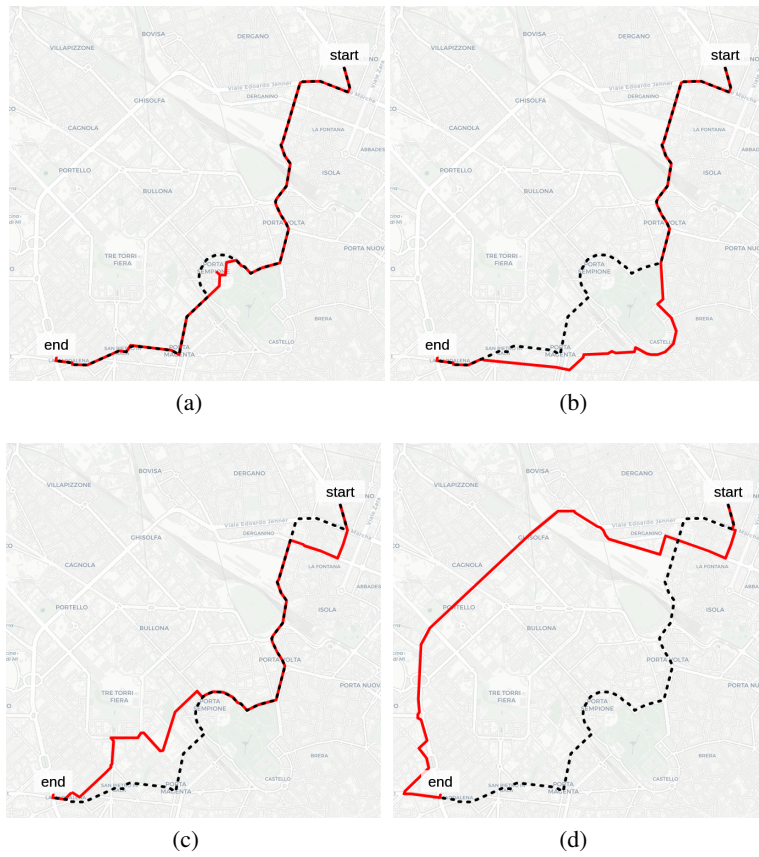


Figure S3: Perturbations (red lines) of the fastest path (black dashed line) for  $w=5$  (a),  $w=10$  (b),  $w=15$  (c), and  $w=20$  (d). Increasing  $w$  produces routes that diverge more from the fastest path.

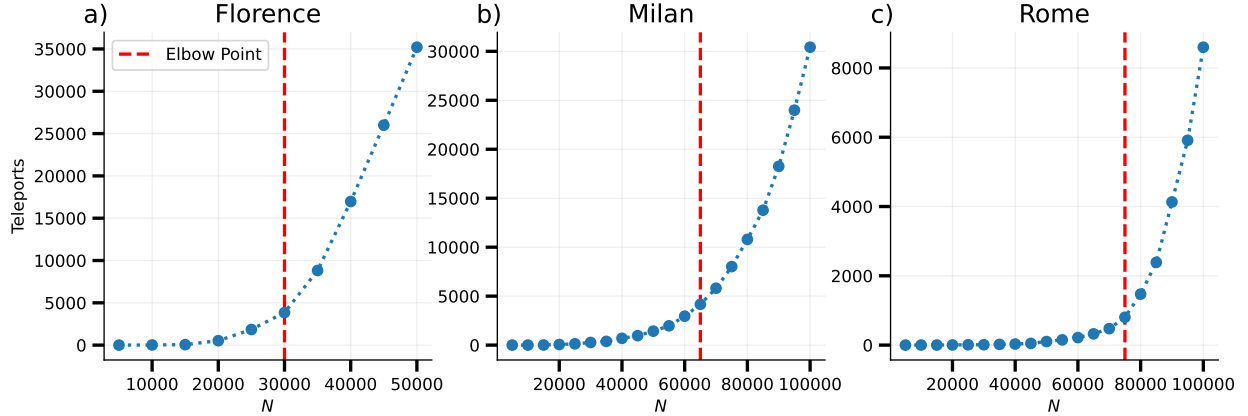


Figure S4: Number of vehicles in the simulation versus the number of SUMO teleports for Florence, Milan, and Rome. Simulations are conducted based on the mobility demand of the city and using the fastest route. The red dashed line denotes the elbow point of the curve.

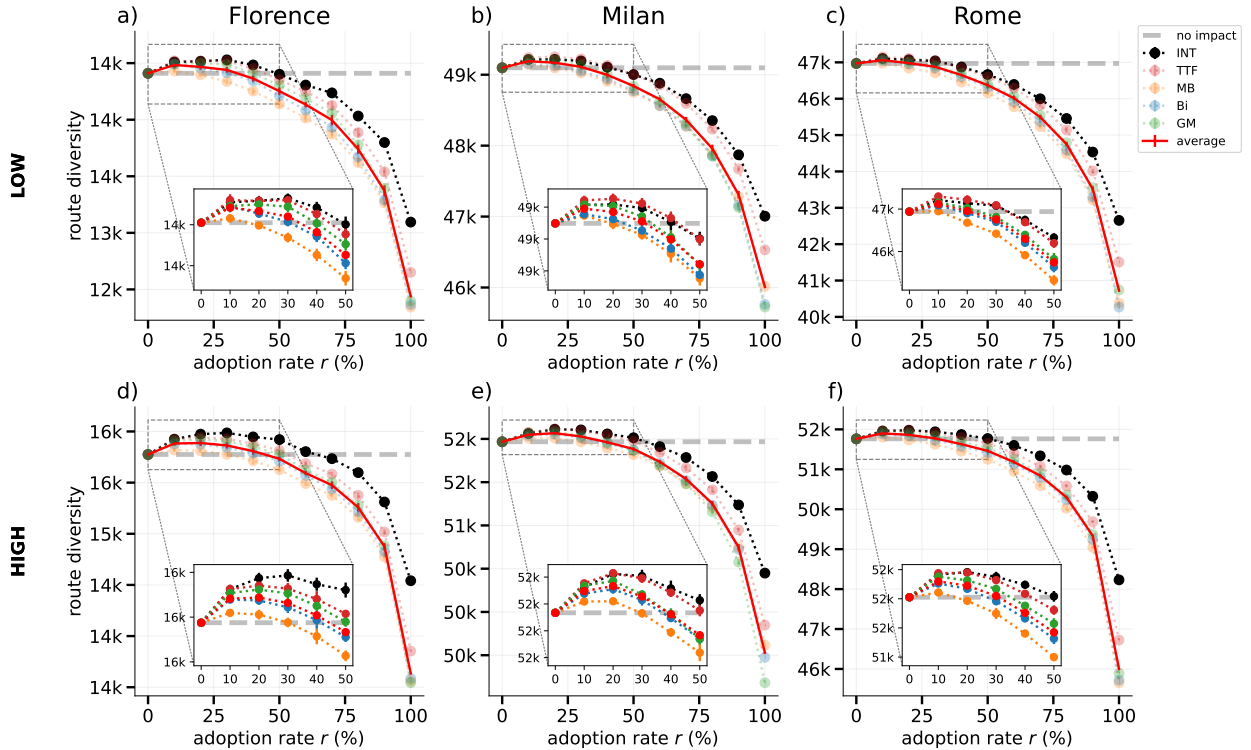


Figure S5: Service adoption rate versus route diversity at low (a-c) and high (d-f) traffic loads in Florence, Milan, and Rome. The dashed line represents the no-impact scenario (adoption rate  $r = 0\%$ ). The black curve represents the market share scenario, while the red curve denotes the average of the curves for individual services (i.e., GM, Bi, MB, TTF). In the error bars, points indicate the average route diversity over ten simulations with different choices of  $s$ -routed vehicles chosen uniformly at random. Vertical bars indicate the standard deviation. The inset plots zoom on the range  $r = 0\%, \dots, 50\%$ , where route diversity slightly increases.

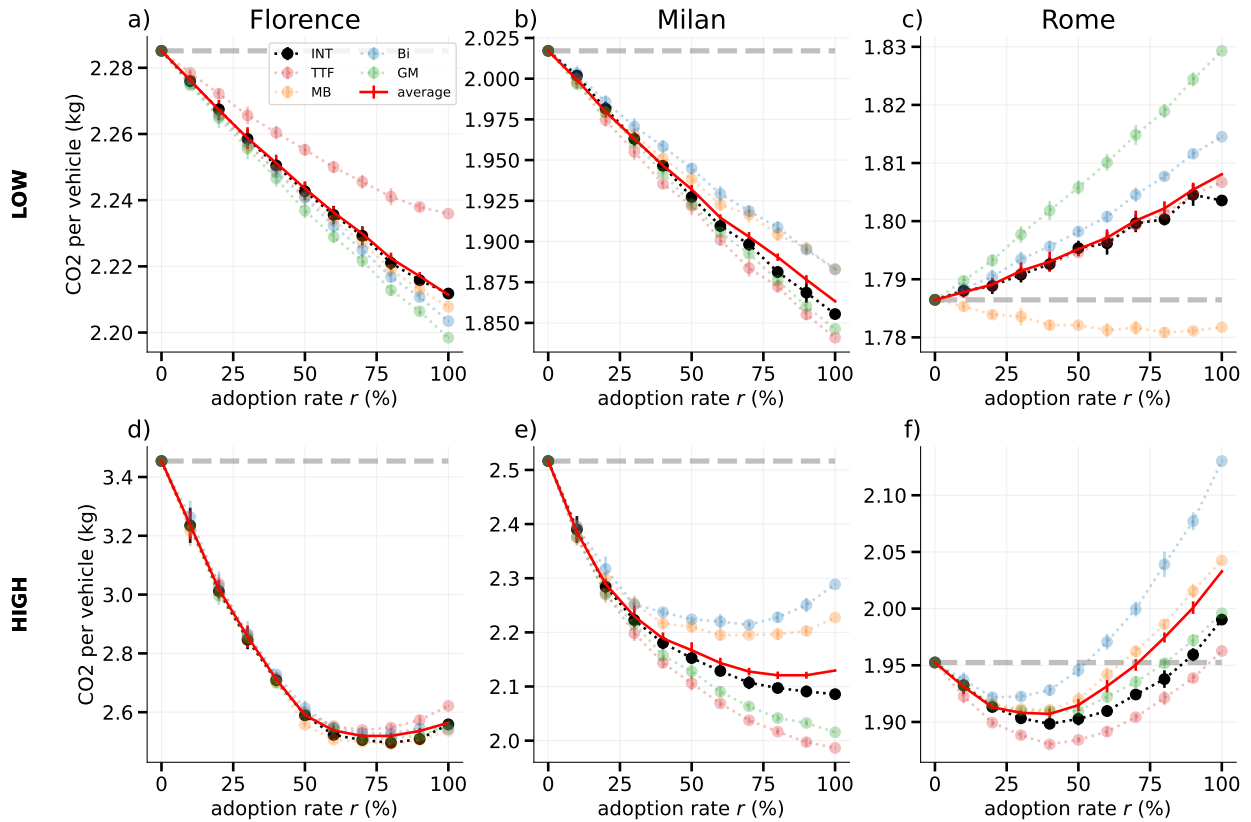


Figure S6: Service adoption rate versus average CO2 emissions per vehicle at low (a-c) and high (d-f) traffic loads in Florence, Milan, and Rome. The dashed line represents the no-impact scenario (adoption rate  $r = 0\%$ ). The black curve represents the market share scenario while the red curve denotes the average of the curves for individual services (i.e., GM, Bi, MB, TTF). In the error bars, points indicate the average CO2 emissions per vehicle over ten simulations with different choices of  $s$ -routed vehicles chosen uniformly at random. Vertical bars indicate the standard deviation.

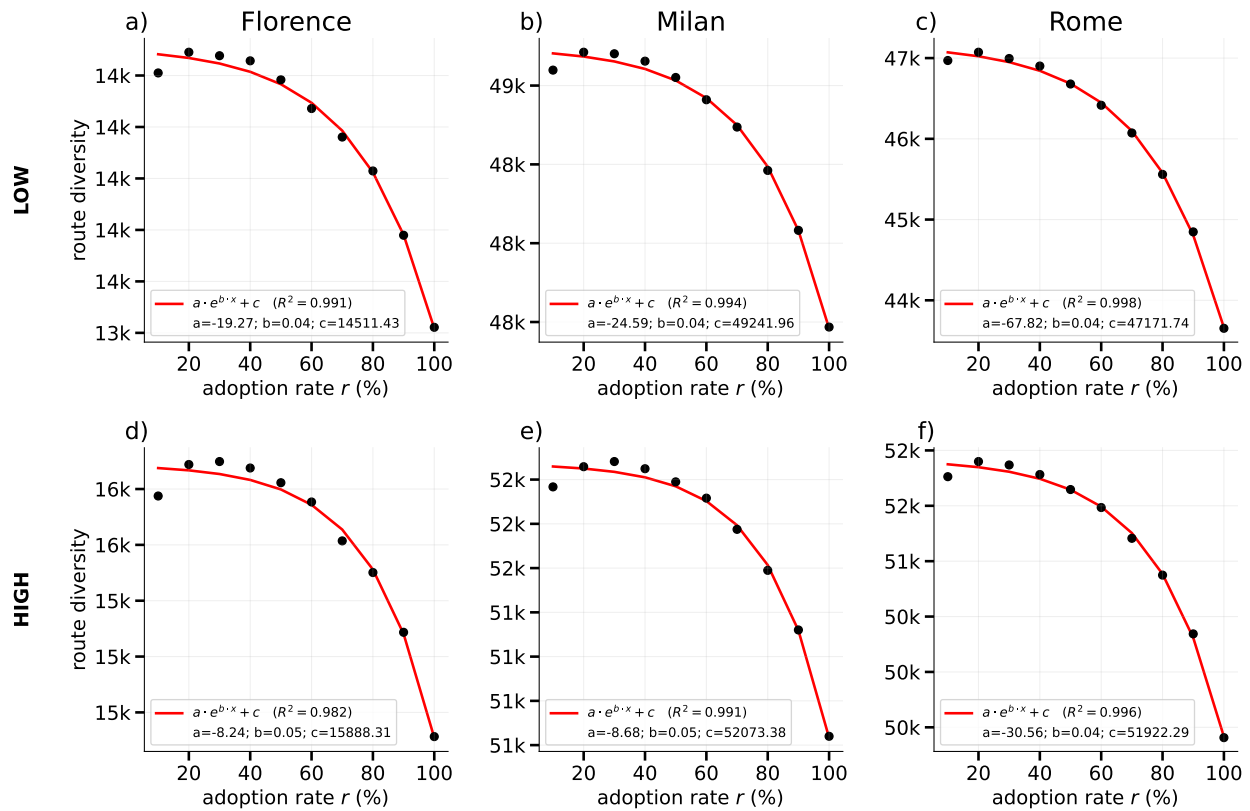


Figure S7: Service adoption rate versus route diversity at low (a-c) and high (d-f) traffic loads in Florence, Milan, and Rome. The data points represent the average route diversity across different navigation systems at varying adoption rates. The red curves illustrate the best-fitting exponential function  $y = a \cdot e^{b \cdot x} + c$ , with the goodness of fit ( $R^2$ ) and the parameter values ( $a$ ,  $b$ ,  $c$ ). The exponential model consistently provides the best fit across all scenarios.

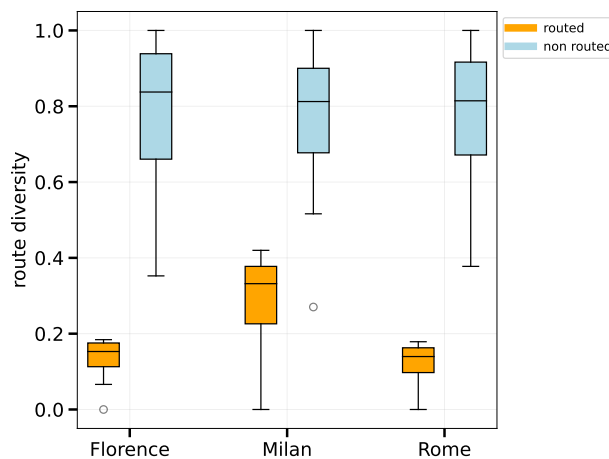


Figure S8: The distribution of the normalized route diversity for routed (orange) and non-routed (blue) vehicle groups across Florence, Milan, and Rome. The routed groups exhibit significantly lower route diversity compared to the non-routed groups, indicating a higher degree of route conformity among vehicles using navigation services.

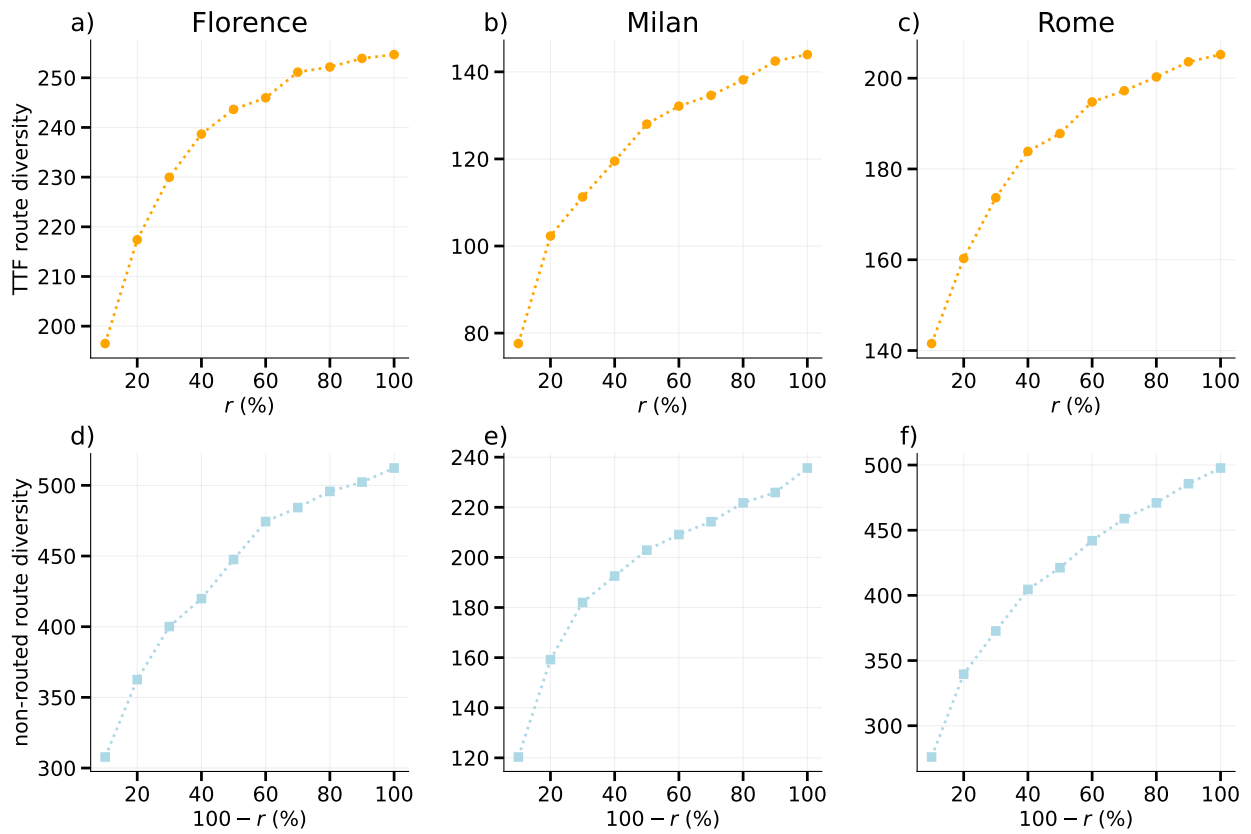


Figure S9: Service adoption rate versus route diversity for TTF-routed (a-c) and non-routed (d-f) vehicle groups. Route diversity increases for both routed and non-routed groups as the number of vehicles in each group increases with their respective adoption rates.

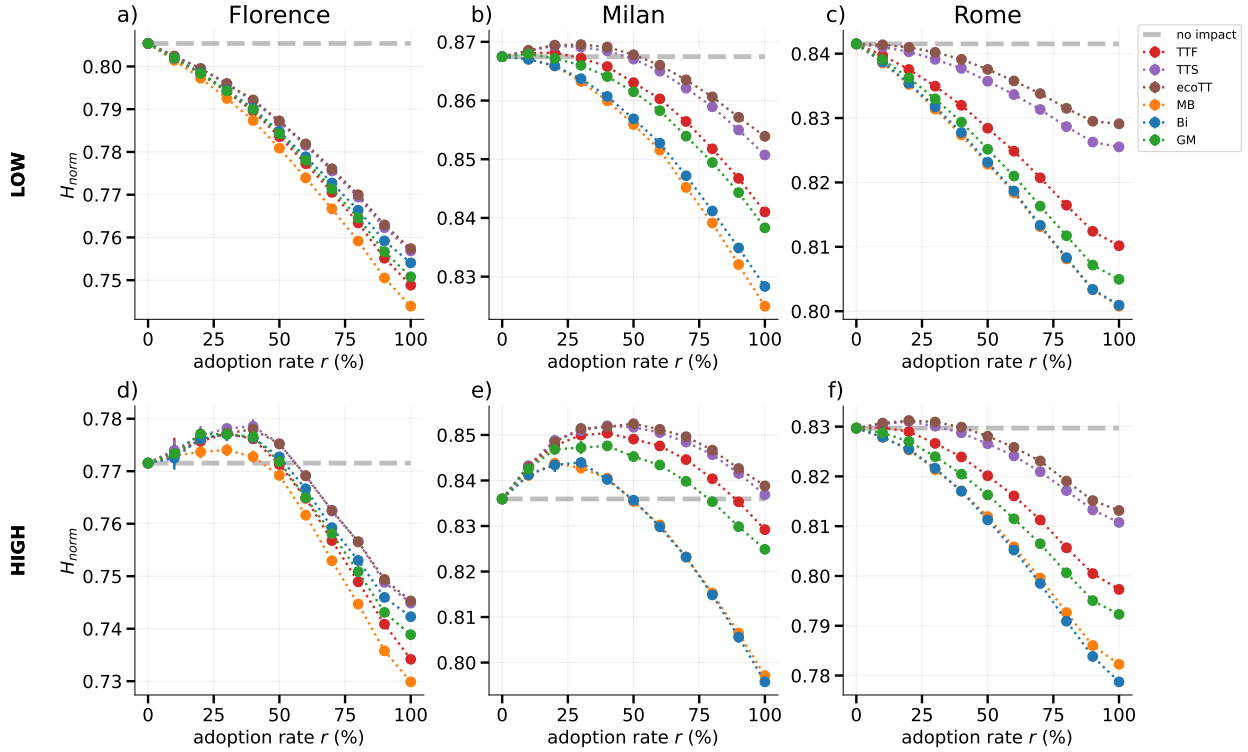


Figure S10: Service adoption rate versus the normalized entropy of CO2 Emissions on roads at low (upper row) and high traffic loads (lower row) in Florence, Milan, and Rome. The dashed line represents the no-impact scenario (adoption rate  $r = 0\%$ ). In the error bars, points indicate the average route diversity over ten simulations with different choices of  $s$ -routed vehicles chosen uniformly at random. Vertical bars indicate the standard deviation.

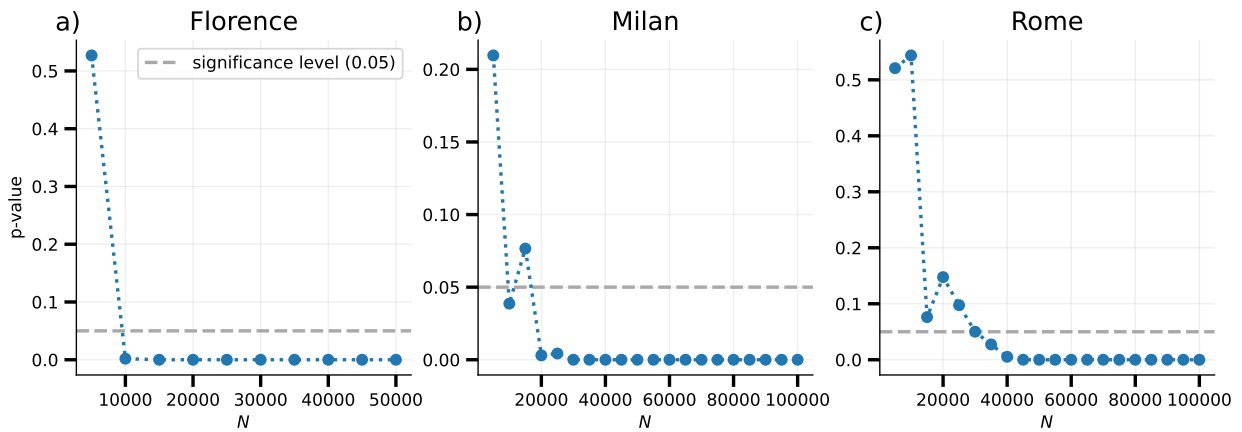


Figure S11: P-value for the exponential fit between the marginal change in route diversity ( $\Delta D_r$ ) and the marginal change in CO2 emissions ( $\Delta E_r$ ) with varying numbers of circulating vehicles ( $N$ ) in Florence, Milan, and Rome. The dashed line represents the 0.05 significance level. The relationship becomes significant ( $p < 0.05$ ) from 10,000 vehicles for Florence, 20,000 for Milan, and 35,000 for Rome, indicating a significant exponential relationship.

## B Supplementary Tables

city	$ V $	$ E $	$\frac{ E }{ V }$	Total Edge Length (km)	Total Lane Length (km)
Florence	11,454	22,728	1.984	2,876	3,264
Milan	29,134	56,521	1.940	5,260	6,324
Rome	32,815	65,352	1.992	6,788	8,301

Table S1: Road network characteristics for the three cities. The columns show the number of vertices  $|V|$  and edges  $|E|$ , their ratio  $\frac{|E|}{|V|}$ , the total edge length (in km), and the total lane length (in km).

		low traffic		high traffic	
		best	100%	best	100%
Florence	Bi	-	3.57%	26.83% (r=80%)	26.40%
	MB	-	3.38%	27.87% (r=80%)	26.56%
	ecoTT	-	5.00%	27.40% (r=80%)	26.76%
	TTF	-	2.15%	26.49% (r=70%)	24.11%
	TTS	-	4.87%	27.55% (r=80%)	26.75%
	GM	-	3.79%	27.33% (r=70%)	26.01%
Milan	Bi	-	6.66%	12.01% (r=70%)	9.05%
	MB	-	6.64%	12.78% (r=60%)	11.48%
	ecoTT	-	11.13%	-	22.13%
	TTF	-	8.73%	-	21.05%
	TTS	-	10.51%	-	22.04%
	GM	-	8.47%	-	19.91%
Rome	Bi	$\emptyset$	-1.57%	1.57% (r=20%)	-9.10%
	MB	0.31% (r=80%)	0.26%	2.14% (r=40%)	-4.61%
	ecoTT	-	3.69%	5.20% (r=70%)	3.69%
	TTF	$\emptyset$	-1.13%	3.70% (r=40%)	-0.52%
	TTS	-	3.09%	4.91% (r=60%)	2.92%
	GM	$\emptyset$	-2.40%	2.21% (r=40%)	-2.22%

Table S2: Reduction in total CO2 emissions for various navigation services in Florence, Milan, and Rome compared to the baseline scenario (no vehicle routed). Positive values indicate a reduction, while negative values indicate an increase. The table includes data for low and high traffic conditions. Values are reported at 100% and at the point of maximum reduction (best), including the percentage of best reduction. In the "best" column, a "-" indicates the maximum reduction is achieved at 100%, and a  $\emptyset$  means the navigation service is never beneficial.

## C Supplementary Notes

### C.1 Supplementary Note 1: Mobility Demand and GPS data

An urban mobility demand  $D$  is a time-ordered collection of trips characterized by their origin, destination, and departure time. To estimate the mobility demand, we rely on the vehicular GPS trajectory dataset provided by Octo, a company that offers a data collection service for insurance companies. This dataset describes the trajectories of thousands of vehicles for various Italian localities over the span of an entire year. While the market penetration of the dataset varies, it generally represents a minimum of 2% of the total registered vehicles.

Our analysis focuses on Florence, Milan, and Rome, chosen due to the availability of GPS traces suitable for computing origin-destination (OD) matrices and their diverse sizes, populations, and road network structures. The raw dataset includes 7,102,351 GPS points from 24,640 vehicles in Florence, 143,698,720 GPS points from 106,456 vehicles in Milan, and 26,801,872 GPS points from 30,763 vehicles in Rome.

We first performed a pre-processing step to extract segmented trajectories representing semantic journeys from the raw GPS dataset. Next, to compute the OD matrix reflecting a city’s traffic patterns, we discretize the city into 1 km<sup>2</sup> squared tiles using scikit-mobility [36]. We then filter and aggregate the segmented trips into flows to derive OD matrices that reflect the cities’ traffic patterns.

**Pre-processing steps.** We pre-process the raw GPS dataset to obtain a collection of segmented trajectories (i.e., trips) by performing the following operations:

- We consider only the GPS points with the maximum sampling quality to ensure the highest accuracy and reliability of the data, reducing the risk of errors due to poor signal quality or inaccurate location measurement;
- We eliminate noise by filtering out GPS points with speeds exceeding 250 km/h [49];
- We use a stop detection algorithm [49] to segment each trajectory into sub-trajectories based on identified stops. A stop is identified when a vehicle remains within a distance of 0.2 km from a trajectory point for at least 20 minutes;
- We considered only trips that both start and end within the predefined area of interest (i.e., the city’s bounding box). For trips that start or end outside this area but traverse it, we used the first entry point within the area as the origin and the last exit point as the destination. This method preserves commuter trips originating or ending outside the city.

**Flow filtering.** To compute the flows from the collection of trips extracted from the raw GPS data, we filter the trips as follows:

- We consider only trips with a duration between 5 and 60 minutes to focus on typical urban commutes. Short trips (less than 5 minutes) often involve anomalies such as GPS errors or very brief stops, which do not provide meaningful data on urban traffic patterns. Conversely, trips longer than 60 minutes may include long-distance travel or other atypical journeys.
- We discard outlier days by analyzing their Pearson correlation with aggregate mobility patterns. Aggregate mobility refers to the sum of all flows within a specific time period. Specifically, we compare the mobility flow of each day to the aggregate mobility flow of all other days that fall on the same day of the week (e.g., comparing all Mondays). A day is classified as an outlier if its correlation with the aggregate mobility flow is below a certain threshold defined as the average correlation minus the standard deviation. By excluding these outlier days, we effectively remove anomalies and inconsistent data, ensuring a more accurate representation of typical mobility patterns.

- We focus exclusively on trips that depart during the morning peak, a period characterized by intense traffic congestion. This time frame offers a robust scenario for analyzing vehicular movement patterns and understanding the impact of navigation services on emissions within typical urban traffic conditions.
- We consider only trips that depart on Wednesdays. Our analysis shows that aggregate mobility during the morning peak hours of weekdays is highly correlated (average Pearson correlation of 0.780 in Florence, 0.880 in Milan, and 0.772 in Rome), indicating that traffic patterns are consistent across working days. In contrast, there is a low correlation between weekend and weekday traffic patterns. We chose Wednesday because it is a mid-week working day, providing a balanced representation of weekly traffic.
- We filter out infrequent flows, retaining only those that occur regularly. We use a data-driven approach to determine the frequency threshold (i.e., the minimum number of trips to define a flow as frequent). We examine the number of non-zero flows across various frequency thresholds and we identify the elbow point of this function, where the number of flows decreases significantly. This elbow point represents the optimal frequency threshold, allowing us to remove noise flows while preserving meaningful data.

After the flow filtering, the datasets used to generate an OD-matrix  $M$  for each city include:

- Florence: 5,477 trips from 1,184 vehicles, resulting in 616 distinct flows;
- Milan: 113,323 trips from 15,997 vehicles, resulting in 11,967 distinct flows.
- Rome: 13,647 trips from 1,965 vehicles, resulting in 1,757 distinct flows.

**Mobility demand generation.** To generate a mobility demand  $D$  consisting of  $N$  trips from the OD matrix  $M$ , we follow these steps to ensure that  $D$  accurately represents the spatial distribution of trips within the city based on the observed data.

- **Random Trip Selection:** For each vehicle  $v$ , we randomly select a trip  $T_v = (e_o, e_d)$ . The origin-destination pair  $(o, d)$  is chosen based on the probabilities  $p_{o,d} \propto m_{o,d}$ , where  $m_{o,d}$  represents the elements of the OD matrix  $M$ . This ensures that trips are selected in proportion to their frequency in the OD matrix;
- **Edge Selection within Tiles:** Once an origin-destination pair  $(o, d)$  is selected, we uniformly choose two edges  $e_o$  and  $e_d$  within the respective tiles  $o$  and  $d$  from the road network  $G$ . This step ensures that the trips are mapped to specific routes within the city’s road network, reflecting realistic travel paths.

## C.2 Supplementary Note 2: Navigation Services APIs

We consider several navigation services with public APIs, including Google Maps (GM), MapBox (MB), Bing Maps (Bi), TomTom fastest route (TTF), TomTom shortest route (TTS), and TomTom eco routing (EcoTT). These services suggest a route between an origin  $o$  and a destination  $d$  at a time  $t$ , considering various factors such as the typical traffic conditions at the time  $t$  when the trip  $(o, d, t)$  departs.

The APIs provide recommendations based on real-time, real-world traffic conditions, which can be influenced by unpredictable events like accidents or construction work. To ensure consistency with our simulated traffic, we request routes for future departure times  $t$  relative to the time of the request, forcing the navigation services APIs to use historical traffic information instead of real-time traffic conditions.

The route recommendations from the APIs are typically provided as sequences of GPS points. We employed a map-matching procedure to integrate these routes into the SUMO simulator. Specifically, we applied the state-of-the-art Longest Common Subsequence (LCSS) algorithm [50] to convert the sequence of GPS points into a sequence of connected edges in the SUMO road network, accurately representing the suggested routes.

Including multiple navigation services allows us to consider different road network representations, routing criteria, and traffic data. These selected services cover a variety of routing criteria, from eco-friendly to the fastest and shortest

routes, offering a comprehensive comparison. We evaluate the similarity among navigation services by calculating the average pairwise overlap among their recommended routes using the Jaccard Index.

Figure S2 shows the average overlap (below the diagonal) and the percentage of exact matches (above the diagonal) of the routes suggested by navigation services. The average overlap ranges from 70 to 97%. Notably, the highest overlaps are associated with TomTom-based services, which share the exact road network representation, differing only in routing criteria. The exact matches between navigation services from different providers do not exceed 50%.

The high overlap observed across all three cities between TomTom’s eco routing (ecoTT) and shortest route (TTS) criteria, defined as trade-offs between travel time and fuel consumption for ecoTT, and travel time and travel distance for TTS, suggests that these criteria lead to similar route recommendations. This indicates that routes optimized for fuel efficiency often align closely with those optimized for minimizing travel distance, especially within the same road network and traffic data context. Overall, these observations underscore the variability and complexity in route recommendations provided by different navigation services, despite some high overlaps among services from the same provider (e.g., TomTom).

### C.3 Supplementary Note 3: Duarouter

To model the imperfections of human driving behavior, which often deviates from the fastest route due to personal preferences, incomplete knowledge of the road network, and irrational behaviors [41, 51], we use the SUMO tool *duarouter*<sup>4</sup>. This tool calculates routes using the Dijkstra algorithm, incorporating a degree of path randomization  $w \in [1, +\infty)$  to increase route variability.

When  $w = 1$ , *duarouter* calculates the standard fastest route on the road network. For  $w > 1$ , *duarouter* applies an edge weight randomization method [14], dynamically altering edge weights (i.e., expected travel time) by a random factor drawn uniformly in  $[1, w)$ . This distortion of edge costs occurs every time *duarouter* computes the fastest path for a vehicle, meaning that two vehicles with the same origin and destination may be assigned to two different randomized fastest paths. *Duarouter* randomizes the edge weight  $t(e)$  (i.e., expected travel time) of an edge  $e$  using a function  $f_{dua}(e)$  defined as:

$$f_{dua}(e) = t(e) \cdot \mathcal{U}(1, w)$$

where  $w$  is the degree of randomization and  $\mathcal{U}(1, w)$  is a random value drawn uniformly in  $[1, w)$ . Note that for  $w = 1$ , there is no randomization. Furthermore, the higher  $w$ , the more randomness is introduced into calculating the fastest path, and the more (on average) the path deviates from the fastest path (see Figure S3). In our study, we set  $w = 5$ , introducing a moderate level of randomness into the computation of the fastest path using *duarouter*.

### C.4 Supplementary Note 4: Traffic Conditions

We employed a data-driven approach for each city to determine the number of vehicles  $N$  corresponding to high and low traffic conditions.

Initially, we analyzed the relationship between the number of teleports and the number of vehicles  $N$  using the fastest path (S4). In this context, a "teleport" refers to a mechanism in SUMO that instantaneously relocates a vehicle stuck in traffic to maintain a smooth simulation flow and prevent deadlocks. It moves vehicles to a point where they can continue their trip. The number of teleports serves as a proxy for traffic congestion. Specifically, the number of teleports represents the average teleports observed in the simulation at a specific  $N$  for adoption rates ranging from 0% to 100%, incremented by 10%.

We identified the elbow point of this function, which indicates the  $N$  value at which the rate of increase in the number of teleports begins to rise sharply, signaling a significant change in congestion levels. This point serves as an ideal

<sup>4</sup><https://sumo.dlr.de/docs/duarouter.html>

indicator for high traffic conditions. To define low traffic conditions, we selected an  $N$  value significantly lower than the elbow point.

The specific  $N$  values for each city and traffic condition are defined as follows:

- **Florence:**  $N=10,000$  for low traffic and  $N=30,000$  for high traffic.
- **Milan:**  $N=30,000$  for low traffic and  $N=65,000$  for high traffic.
- **Rome:**  $N=25,000$  for low traffic and  $N=75,000$  for high traffic.

### C.5 Supplementary Note 5: Simulation of Market Share

Our primary study examined the influence of individual navigation services on urban traffic in isolation. However, as vehicles in real cities use a mix of these services, we extended our analysis to include a scenario where vehicles could choose among multiple services. We simulated scenarios in which each navigation service (GM, Bi, MB, TTF) had an equal market share, i.e., 25%, due to the lack of specific market share data for the services in the selected cities. Given an adoption rate of  $r$ , we randomly assigned  $\frac{r}{4}$  of the vehicles to each navigation service. This approach allowed us to create a more realistic model of how navigation services might interact in guiding traffic within a city.

Our findings from these extended simulations showed that the aggregate impact of using multiple navigation services was similar to the results observed when using single services in isolation. Specifically, the overall route diversity presents the same decreasing trend. However, the drop-off in route diversity at 100% adoption was less severe than single navigation services (see Figure S5). This is because the combination of multiple suggestions from various navigation services covered a larger extent of edges due to the difference in route service recommendations. The CO2 emissions trends were consistent with the single-service scenario. In particular, the trend observed in the interplay of multiple navigation services resembled an average of the curves for individual services (see Figure S6).

### C.6 Supplementary Note 6: Impact Measures

We measure the impact of navigation services on the urban environment in terms of route diversity, i.e., the number of road edges traversed at least once by any vehicle, and the total CO2 emissions per vehicle.

**Route diversity.** We measure the route diversity of a set of routes  $R$  by counting the number of distinct road edges traversed by at least one vehicle. Higher route diversity indicates a greater variety of routes being explored, which typically results in improved traffic distribution and reduced congestion. Conversely, a low route diversity value suggests conformist behavior in the routing process, leading to route convergence and increased traffic concentration.

Formally, given a set of routes  $R$  and a set of edges in these routes, we define its route diversity as:

$$RD(R) = \left| \bigcup_{r \in R} \{e \in r\} \right|$$

**CO2 emissions.** The CO2 emissions are computed using a SUMO functionality that uses the HBEFA3/PC\_G\_EU4 emission model [24], which estimates the vehicle's instantaneous emissions at a trajectory point  $j$  as [27]:

$$\mathcal{E}(j) = c_0 + c_1sa + c_2sa^2 + c_3s + c_4s^2 + c_5s^3$$

where  $s$  and  $a$  are the vehicle's speed, and acceleration in point  $j$ , respectively, and  $c_0, \dots, c_5$  are parameters changing per emission type and vehicle taken from the HBEFA database.

While CO2 emissions are undeniably a vital aspect to consider in the context of impact on the urban environment, they are just one of the several adverse factors exacerbated by vehicular traffic. Other factors such as fuel consumption, NOx

emissions, PM emissions, and acoustic noise also play a crucial role in understanding the overall environmental impact of navigation services. However, we find that these factors are highly correlated among them and with CO2 emissions, both when considering measures on each edge of the road network and for each vehicle (Pearson correlation  $r > 0.994$ , for all cities and navigation services). Consequently, for simplicity, in the paper we present results for CO2 emissions only.

### C.7 Supplementary Note 7: Route Diversity Curve Fitting

We investigate the relationship between the adoption rate and route diversity, defined as the number of traveled edges. Our aim is to identify the most appropriate curve model to represent these relationships. We consider several models: linear ( $y = ax + b$ ), quadratic ( $y = ax^2 + bx + c$ ), cubic ( $y = ax^3 + bx^2 + cx + d$ ), and exponential ( $y = a \cdot e^{b \cdot x} + c$ ). For each city, we calculate the average route diversity across different navigation systems at varying adoption rates and fit the data using these models. This analysis is performed under both low and high traffic conditions. The goodness of fit for each model is evaluated using the  $R^2$  metric. Our findings indicate that the exponential function consistently provides the best fit across all cities and traffic scenarios. Figure S7 illustrates the average route diversity alongside the best-fitting function.

### C.8 Supplementary Note 8: Route Diversity in the Treatment and Control Groups

We investigate how route diversity, defined as the number of distinct road segments traversed, varies between treatment ( $s$ -routed) and control (non- $s$ -routed) groups. Specifically, we focus on the top 30 most traveled flows within each city and examine the impact of varying the adoption rate  $r$  of navigation services from 0% to 100% in 10% increments. We compute the normalized average route diversity for the treatment and control groups for each adoption rate.

Our results reveal a significant reduction in route diversity for the routed group compared to the control group, as illustrated in the box plot in Figure S8. This suggests vehicles following navigation service recommendations converge on fewer routes, leading to increased route conformity. Moreover, we analyze the trend in route diversity as the number of vehicles in the control and treatment groups increases (see Figure S9). Our findings show that although both groups exhibit an increasing trend in route diversity with higher vehicle numbers, the increase is more pronounced for non-routed vehicles.

### C.9 Supplementary Note 9: Inequality of Distribution of CO2 Emissions on Roads

Under certain circumstances, navigation services can decrease or plateau CO2 emissions as their adoption rate increases. However, with higher adoption rates, CO2 emissions become concentrated on a smaller fraction of roads due to increased route conformity, thereby increasing the inequality in the distribution of CO2 emissions on the road network.

To demonstrate that high adoption rates generate inequality in CO2 emissions, we examine how the entropy—a measure of distribution uniformity—of CO2 emitted on each road edge changes with varying adoption rates of navigation services. Entropy  $H$  is computed as:

$$H = - \sum_i p_i \log p_i$$

where  $p_i$  is the proportion of CO2 emissions on road edge  $i$ . The normalized entropy  $H_{\text{norm}}$  is then calculated considering the total number of edges ( $E$ ) as:

$$H_{\text{norm}} = \frac{H}{\log E}$$

We tested the entropy calculations with and without including edges with no associated emissions, and the results are essentially the same. Our findings indicate that, under both low and high traffic conditions, as adoption rates  $r$  increase, the normalized entropy decreases in Florence, Milan, and Rome, signaling a less uniform distribution of CO2 emissions (Figure S10). This unequal CO2 distribution may exacerbate air quality issues in specific neighborhoods, increase exposure to harmful pollutants for residents in those areas, and strain local infrastructure. While navigation services can reduce emissions at lower adoption rates, widespread use without strategic management can lead to significant inequalities in emission distribution.

### C.10 Supplementary Note 10: Exponential Relationship Between $\Delta D_r$ and $\Delta E_r$

We investigated how the exponential relationship between the marginal change in route diversity ( $\Delta D_r$ ) and the marginal change in CO2 emissions ( $\Delta E_r$ ) is influenced by the number of circulating vehicles ( $N$ ). For each city, we computed the  $p$ -value associated with the exponential fit between  $\Delta D_r$  and  $\Delta E_r$  for various values of  $N$  (Figure S11). The  $p$ -value indicates the significance of the exponential fit, with lower  $p$ -values signifying a more stable and significant relationship. We selected a significance level of 0.05 for our analysis. The fit is represented by the exponential decay function  $\Delta E_r = \alpha e^{-\beta \Delta C_r} + \gamma$ . The statistical hypotheses are:

- Null Hypothesis (H0): There is no significant exponential relationship between  $\Delta D_r$  and  $\Delta E_r$ .
- Alternative Hypothesis (H1): There is a significant exponential relationship between  $\Delta D_r$  and  $\Delta E_r$ .

In all cities, the null hypothesis (H0) is rejected in favor of the alternative hypothesis (H1) when the number of circulating vehicles exceeds the identified thresholds, as indicated by  $p$ -values below the significance level of 0.05. The city-specific thresholds, defined as the first  $N$  for which the relationship becomes significantly exponential, are 10,000 for Florence, 20,000 for Milan, and 35,000 for Rome.